

Article

Deciphering the Prognostic Efficacy of MRI Radiomics in Nasopharyngeal Carcinoma: A Comprehensive Meta-Analysis

Chih-Keng Wang ^{1,2,†}, Ting-Wei Wang ^{1,3,†} , Chia-Fung Lu ⁴ , Yu-Te Wu ^{3,*}  and Man-Wei Hua ^{2,*}¹ School of Medicine, College of Medicine, National Yang-Ming Chiao Tung University, Taipei 112304, Taiwan² Department of Otolaryngology-Head and Neck Surgery, Taichung Veterans General Hospital, Taichung 407219, Taiwan³ Institute of Biophotonics, National Yang-Ming Chiao Tung University, 155, Sec. 2, Li-Nong St. Beitou Dist., Taipei 112304, Taiwan⁴ Department of Biomedical Imaging and Radiological Sciences, National Yang-Ming Chiao Tung University, Taipei 112304, Taiwan; alvin4016@ym.edu.tw

* Correspondence: ytwu@nycu.edu.tw (Y.-T.W.); ppmabcde@hotmail.com (M.-W.H.); Tel.: +886-2-2826-7000 (ext. 5707) (Y.-T.W.); +886-9-1013-3171 (M.-W.H.)

† These authors contributed equally to this work.

Abstract: This meta-analysis investigates the prognostic value of MRI-based radiomics in nasopharyngeal carcinoma treatment outcomes, specifically focusing on overall survival (OS) variability. The study protocol was registered with INPLASY (INPLASY202420101). Initially, a systematic review identified 15 relevant studies involving 6243 patients through a comprehensive search across PubMed, Embase, and Web of Science, adhering to PRISMA guidelines. The methodological quality was assessed using the Quality in Prognosis Studies (QUIPS) tool and the Radiomics Quality Score (RQS), highlighting a low risk of bias in most domains. Our analysis revealed a significant average concordance index (c-index) of 72% across studies, indicating the potential of radiomics in clinical prognostication. However, moderate heterogeneity was observed, particularly in OS predictions. Subgroup analyses and meta-regression identified validation methods and radiomics software as significant heterogeneity moderators. Notably, the number of features in the prognosis model correlated positively with its performance. These findings suggest radiomics' promising role in enhancing cancer treatment strategies, though the observed heterogeneity and potential biases call for cautious interpretation and standardization in future research.



Citation: Wang, C.-K.; Wang, T.-W.; Lu, C.-F.; Wu, Y.-T.; Hua, M.-W. Deciphering the Prognostic Efficacy of MRI Radiomics in Nasopharyngeal Carcinoma: A Comprehensive Meta-Analysis. *Diagnostics* **2024**, *14*, 924. <https://doi.org/10.3390/diagnostics14090924>

Received: 25 February 2024

Revised: 12 April 2024

Accepted: 24 April 2024

Published: 29 April 2024



Copyright: © 2024 by the authors. Licensee MDPI, Basel, Switzerland. This article is an open access article distributed under the terms and conditions of the Creative Commons Attribution (CC BY) license (<https://creativecommons.org/licenses/by/4.0/>).

Keywords: radiomics; prognostic models; meta-analysis; survival

1. Introduction

Nasopharyngeal carcinoma (NPC) exhibits notable epidemiological differences globally, with a significantly higher incidence in East and Southeast Asia compared to Western countries. These disparities are attributed to genetic susceptibility, environmental factors, and Epstein-Barr virus (EBV) infection prevalence. The distinct epidemiological patterns of NPC necessitate tailored approaches in diagnosis, treatment, and prognosis across different populations [1,2]. In pursuing personalized medicine, radiomics and machine learning have emerged as transformative tools, offering new avenues for the prognostic assessment of NPC [3,4].

Radiomics involves extracting high-dimensional data from medical images, which, when analyzed through machine learning algorithms, can reveal patterns indicative of tumor phenotype, aggressiveness, and likely response to treatment. This methodology extends the value of conventional MRI scans beyond anatomical visualization, enabling the quantification of tumor heterogeneity at a microscopic level that may not be visually apparent [5,6]. Machine learning further enhances this process by identifying complex relationships between radiomic features and clinical outcomes, facilitating the development of predictive models for NPC prognosis [7,8].

The integration of radiomics and machine learning in NPC research holds the potential to revolutionize patient care. By accurately predicting treatment outcomes, these technologies can guide the selection of therapeutic strategies tailored to individual patient profiles, thus improving survival rates and quality of life. Moreover, the ability to monitor tumor response non-invasively through advanced imaging analytics could lead to more dynamic and responsive treatment plans, adjusting to changes in tumor behavior over time [9–12].

Despite the promising prospects of radiomics and machine learning in enhancing the prognosis of nasopharyngeal carcinoma (NPC), significant challenges in the standardization of image acquisition, feature extraction, and model validation persist. These hurdles must be overcome to fully leverage the clinical potential of these advanced technologies. A recent meta-analysis highlighted the efficacy of MRI radiomics in predicting the progression-free survival in NPC, presenting a pooled concordance index (C-index) of 0.762 (95% CI, 0.687–0.837) [13]. However, this analysis also noted a high level of heterogeneity ($I^2 = 89%$) due to the amalgamation of various endpoints, such as Local Recurrence-Free Survival, Distant Metastasis-Free Survival, and Progression-Free Survival. Our research aims to provide an updated synthesis of the current evidence while offering separate analyses for different endpoints. This approach intends to deliver a more nuanced and comprehensive analysis, potentially reducing heterogeneity and enhancing the interpretability of radiomics in the prognosis of NPC.

2. Materials and Methods

This investigation was executed adhering to the Preferred Reporting Items for Systematic Reviews and Meta-Analyses (PRISMA) guidelines for meta-analysis [14]. The PRISMA checklists can be found in Supplemental Table S1. Registration of the study was completed in INPLASY with the registration number INPLASY202420101. It was determined that approval from an ethical review board or obtaining participant informed consent was not requisite for this study.

2.1. Database Searches and the Identification of Eligible Manuscripts

Two independent researchers (C-KW and T-WW) conducted an exhaustive literature review, employing a detailed search strategy across PubMed, Embase, and Web of Science, as outlined in Supplementary Table S2. This review spanned the inception of these databases to 17 February 2024. Articles were systematically screened for relevance based on titles and abstracts, with the inclusion and exclusion criteria established collaboratively. Reference lists of key review articles, including [13], were examined to ensure completeness and supplemented by manual searches to capture any overlooked studies. Discrepancies regarding study inclusion were resolved through consultation with a third investigator.

2.2. Inclusion and Exclusion Criteria

The inclusion criteria were specified for participants definitively diagnosed with nasopharyngeal carcinoma (NPC), focusing exclusively on adult populations of both sexes. The required imaging criteria stipulated that subjects must have undergone magnetic resonance imaging (MRI) for initial radiomic assessment. This criterion applied to both individuals receiving a new diagnosis and those previously subjected to medical interventions such as surgery, radiation, or chemotherapy. Only studies that included the concordance index (c-index) were considered. The c-index, a measure of the prognostic accuracy of models in time-to-event analysis where data may be censored, was selected based on its utilization in prior research [15], owing to its advantage in providing consistent results across studies with variable endpoints, in contrast to the time-independent area under the curve (AUC) which may lead to heterogeneous outcomes. All observational studies, including retrospective or prospective studies, were included.

The exclusion criteria were established: studies concerning cancers other than NPC; research employing deep learning-based radiomics, attributed to its lower interpretability; research incorporating multiple timepoint radiomics; individual radiomics feature predic-

tion of prognosis without intergradation with a model; radiomics models incorporating clinical features, not radiomics studies; overlapping datasets; and documents in letters, conference proceedings, retracted papers, or those devoid of images. Further, studies using imaging modalities other than MRI, covering topics or outcomes irrelevant to the study aims, presenting data unsuitable for quantitative analysis, or not reporting the c-index were excluded.

2.3. Methodological Quality Appraisal

The methodological integrity of each study incorporated in the analysis was meticulously assessed via two established instruments: the Quality in Prognosis Studies (QUIPS) tool and the Radiomics Quality Score (RQS) [16,17]. The Quality in Prognosis Studies (QUIPS) tool is employed to rigorously assess the risk of bias across various domains in prognostic studies, each evaluated with specific criteria to ascertain the risk level. Study Participation examines how representative the sample is of the target population, focusing on recruitment efficacy and the demographic and clinical similarity to the broader population. Study Attrition assesses the completeness of the follow-up, scrutinizing follow-up rates and the reasons for dropout to determine potential biases if outcomes for those lost differ from those who completed the study. Prognostic Factor Measurement evaluates the accuracy and consistency with which prognostic factors are measured across participants, emphasizing the method's reliability and uniform application. Outcome Measurement investigates the reliability and validity of outcome assessments, ensuring clarity in definitions and uniformity in measurement methods. Study Confounding involves identifying and adjusting for potential confounders, assessing the adequacy of their measurement and control. Statistical Analysis and Reporting reviews the appropriateness of statistical methods and the integrity of result reporting. Each domain's risk of bias is rated as low, moderate, or high, guiding the overall evaluation of a study's methodological soundness and result reliability.

The RQS, tailored for scrutinizing radiomics research, comprises 16 elements to assess the research's reliability and susceptibility to bias. Each element within a study was evaluated and scored, leading to an aggregate score representing the sum of scores across all components, reflecting the overall methodological quality of the radiomics studies under review.

2.4. Definitions of Prognostic Endpoints

Local Recurrence-Free Survival (LRFS): Constitutes a composite metric evaluating the efficacy of therapeutic interventions in maintaining control at both the primary tumor site and regional levels.

Distant Metastasis-Free Survival (DMFS): Denotes the interval from the commencement of therapeutic measures to the first instance of distant metastasis or death, whichever occurs first, indicating the treatment's capacity to inhibit tumor dissemination to distal anatomical sites.

Progression-Free Survival (PFS), Disease-Free Survival (DFS), and Failure-Free Survival (FFS): Although these terms are sometimes utilized interchangeably within the oncological lexicon, they predominantly refer to the duration from treatment initiation to the onset of tumor progression, recurrence, or mortality. These measures are critical for assessing the period during which a patient remains unaffected by worsening or reemergence of the disease. For the objectives of this research, these indicators are collectively considered under the umbrella of PFS.

Overall Survival (OS): This parameter measures the time elapsed from the beginning of treatment to death attributable to any cause, serving as a fundamental criterion for evaluating the overall effectiveness of cancer treatment modalities.

2.5. Data Extraction and Management

Data extraction was carried out independently by two authors (C-KW and T-WW), encompassing demographic details, study methodology, and specifics of MRI imaging, as well as radiomics and prognostic model characteristics. This process of data collection, conversion, and amalgamation of the results was executed in alignment with the guidelines stipulated in the Cochrane Handbook for Systematic Reviews of Prognosis Studies and pertinent previous studies.

2.6. Statistical Analysis

To address the variability inherent in the studies selected, we employed a random-effects meta-analytical model [18], with statistical significance predetermined at a p -value of less than 0.05 (two-tailed). Our findings were visually synthesized in forest plots. During the preliminary exploration phase, we incorporated all outcomes associated with radiomics across various endpoints. The analysis was stratified according to specific endpoints (LRFS, DMFS, PFS, and OS). Concordance indices derived from composite models (those incorporating radiomic features in conjunction with clinical or other model variables) were excluded from the analysis due to the inclusion of varying clinical features across studies, which may introduce substantial heterogeneity [13]. Sensitivity analysis was carried out with the leave-one-out method. In a more focused secondary analysis, attention was narrowed to the Overall Survival endpoint, recognizing its heterogeneity across the studies. Subgroup analyses were conducted based on geographical location (Asian versus Europe), validation methodology (internal validation versus external validation), MRI sequence (single versus multiple), and radiomics software (in-house versus Pyradiomics), alongside meta-regressions on publication year, training sample size, and the number of features used. The consistency of results across the studies was assessed using the Q-test, with a p -value less than 0.05 indicating significant heterogeneity. The extent of this heterogeneity was evaluated using I^2 metrics, categorized as negligible (0–25%), low (26–50%), moderate (51–75%), or high (76–100%) [19]. Vigilance for potential publication bias was maintained, employing the Egger's method as a diagnostic tool for identifying asymmetry in funnel plots [20]. All statistical analyses were conducted utilizing STATA software (Stata/SE 18.0 for Mac).

3. Results

3.1. Study Identification and Selection

Figure 1 displays the PRISMA flow diagram, outlining our systematic review and selection methodology. Initially, 495 studies were identified across multiple databases: 122 from PubMed, 237 from EMBASE, and 136 from Web of Science. The removal of 230 duplicates left 265 articles for initial review. Using Endnote, titles and abstracts were assessed, excluding 151 articles. The remaining 114 articles underwent thorough full-text evaluation. The allocation of articles from each database and the refinement process to identify relevant studies are detailed in Table S2. After comprehensive analysis, 15 studies were included in our meta-analysis [21–35], with the exclusion rationale documented in Table S3 [8,10,34,36–130].

3.2. Basic Characteristics of Included Studies

A total of 15 studies involving 6243 patients were included. Among these, the majority were conducted in China, with one study from Thailand [21] and another from Italy [32]. The endpoint measures included Local Recurrence-Free Survival (LRFS), Distant Metastasis-Free Survival (DMFS), Progression-Free Survival (PFS), Disease-Free Survival (DFS), Time to Treatment Failure (TTF), and Overall Survival (OS). For details on validation methods, study design, duration, patient demographics, staging, and treatment, refer to Table 1. Information on MRI protocols, such as slice thickness, magnetic field strength, sequences, and scanner types, is available in Table 2. Details on tumor segmentation soft-

ware, annotators, radiomics software, features, prognostic models, and performance are provided in Table 3.

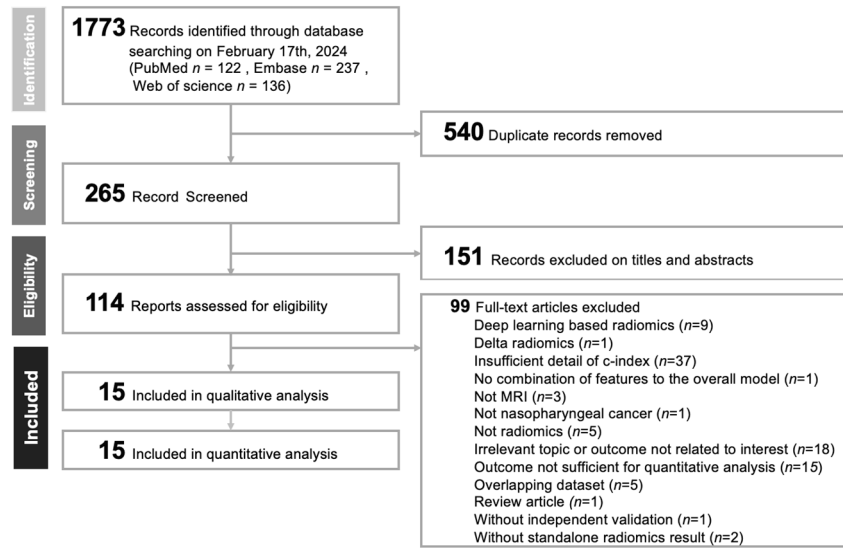


Figure 1. PRISMA flowchart for the current meta-analysis.

3.3. Methodological Quality of the Included Studies

In assessing the methodological quality of the included studies, we found that the majority exhibited a low risk of bias in the sample size domain as per the Quality in Prognosis Studies (QUIPS) tool. However, approximately 13.3% (2 out of 15) demonstrated some risk of bias in the study attrition domain, and nearly 46.7% (7 out of 15) showed some risk in the confounding domain (see Figure 2). Studies identified as having some risk of bias exhibited protocol variations, potentially influencing the adherence to and outcomes of the prognostic models. Detailed assessments of bias risk using QUIPS and the Radiomics Quality Score (RQS) are documented in Tables S4 and S5.

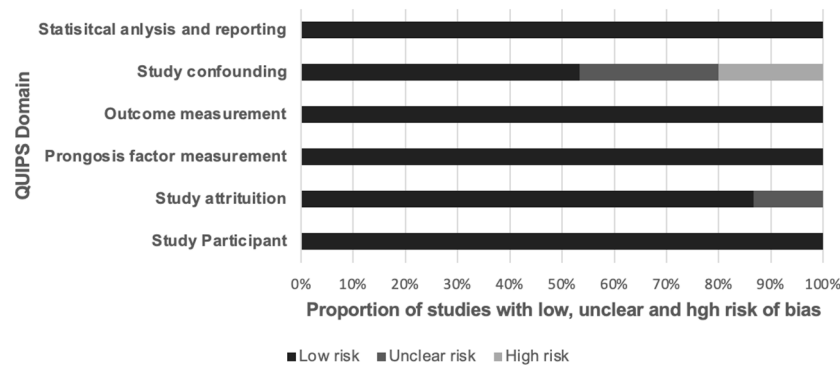


Figure 2. The results of QUIPS quality assessment for included studies.

3.4. Primary Outcome: Overall Radiomics Prognosis Model Performance

In our evaluation of 37 radiomics prognostic outcomes, we observed a concordance index (c-index) ranging from 54% to 81%. The average c-index was a robust 72% (95% Confidence Interval (CI): 70–74%), as depicted in Figure 3. The Q-test yielded a 129.43 ($p < 0.01$), indicating significant heterogeneity. The Higgins I^2 statistic confirmed moderate heterogeneity, accounting for 64.44% variance, further supported by our sensitivity analysis (Figure S1). The Egger test showed no significant publication bias ($p = 0.14$), as illustrated in the funnel plot (Figure S2). Subgroup analysis revealed significant differences ($p = 0.03$) across endpoints.

Table 1. Basic characteristics of studies.

| Author | Geographic | Validation Method | Study Design | Study Duration | Patients (Train/Valid) | Age | Sex (Male) | Stage | Treatment | Endpoint |
|-----------------------------------|------------|---------------------|---------------|----------------|------------------------|---|---|---------|---------------------------|---------------------|
| Khongwirotphan et al. (2024) [21] | Thailand | Internal validation | Retrospective | 2010~2019 | 183 (146/37) | 50 (42.5–57.5)—median/IQR | 143 (78.14%) | I~IVA | IMRT, IMRT + AC | DMFS, PFS, OS |
| Qihao Zhang et al. (2023) [22] | China | Internal validation | Retrospective | 2018~2020 | 151 (75/76) | Train: 52.0 ± 11.2; Test: 49.1 ± 11.4—mean/std | Train: 56 (74.7%); Test: 58 (76.3%) | I~IV | IMRT | PFS |
| Jiang Zhang et al. (2023) [23] | China | External validation | Retrospective | 2013~2019 | 469 (286/183) | Train: 53; Test: 55—median | Train: 216 (75.5%); Test: 143 (78.1%) | II~IV | CCRT | DFS |
| Li et al. (2023) [24] | China | Internal validation | Retrospective | 2018~2021 | 145 (102/43) | Train: 49 (42–57); Test: 51 (40–57)—median | Train: 75 (73.5%); Test: 29 (67.4%) | I~IV | IMRT | PFS |
| Hu et al. (2023) [25] | China | External validation | Retrospective | 2008~2017 | 1072 (575/497) | Train: 44 (38–51); Test: 48 (40–56)—median | Train: 395 (68.7); Test: 326 (65.6) | II | IMRT | DMFS |
| Shen et al. (2022) [26] | China | External validation | Retrospective | 2013~2016 | 893 (390/503) | Train: 48.0 (40.0–56.3); I: 48.0 (40.5–57.5); E1: 47.0 (42.0–53.0); E2: 49.0 (40.0–57.0); E3: 48.0 (42.0–54.0)—median | Train: 276 (70.8); I: 98 (76.0); E1: 76 (73.8); E2: 101 (71.6); E3: 94 (72.3) | III~IVA | IC + CCRT or CCRT + AC | PFS, LRFS, DMFS, OS |
| Liu et al. (2022) [27] | China | Internal validation | Retrospective | 2013~2021 | 504 (353/151) | Train: 49.22(9–85); Test: 47.59(10–80)—mean/range | Train: 243 (68.8); Test: 106 (70.2) | I~IVA | IC, CCRT | OS |
| Li et al. (2022) [28] | China | Internal validation | Retrospective | 2010~2012 | 778 (518/260) | Train: 44 (38–53); Test: 46 (38–52)—median/IQR | Train: 371 (71.6%); Test: 194 (74.6%) | I~IVA | RT alone, CCRT, IC + CCRT | DMFS |
| Jiang et al. (2022) [29] | China | Internal validation | Retrospective | 2015~2017 | 218 (173/45) | 46.1 ± 11.4—mean/std | 164 (75.2%) | I~IV | IC, CCRT, AC | OS |

Table 1. Cont.

| Author | Geographic | Validation Method | Study Design | Study Duration | Patients (Train/Valid) | Age | Sex (Male) | Stage | Treatment | Endpoint |
|----------------------------|------------|---------------------|---------------|----------------|------------------------|--|--|--------|--|---------------|
| Gao et al. (2021) [30] | China | Internal validation | Retrospective | 2012~2014 | 316 (237/79) | NR | Train: 164 (69.2%); Test: 56 (70.9%) | III~IV | Concurrent radical chemoradiotherapy | PFS |
| Zhang et al. (2020) [31] | China | External validation | Retrospective | 2014~2017 | 220 (132/88) | Train: 48 (19–83); I: 49 (27–78); E: 44 (24–70)—median (range) | Train: 96 (72.73%); I: 33 (75.00%); E: 31 (70.45%) | I~IV | Definitive-intent radiotherapy | FFS |
| Bologna et al. (2020) [32] | Italy | Internal validation | Retrospective | 2004~2017 | 136 (122/14) | 48 (39–57)—median (IQR) | 95 (70%) | I~IV | RT alone, Concomitant CHT-RT, Induction CHT + concomitant CHT-RT | OS, PFS, LRFS |
| Zhang et al. (2019) [33] | China | External validation | Retrospective | 2009~2015 | 737 (360/377) | NR | Train: 270 (75.0); I: 90 (75.0); E: 193 (75.1) | I~IV | IMRT, CCRT with or without IC/AC | LRFS |
| Ming et al. (2019) [34] | China | Internal validation | Retrospective | 2010~2012 | 303 (200/103) | 48.8 ± 12.7—mean (std) | 226 (75%) | I~IV | NR | DFS, OS, DMFS |
| Zhang et al. (2017) [35] | China | Internal validation | Retrospective | 2007~2013 | 118 (88/30) | 43 ± 10.98—mean (std) | 92 (0.78) | III~IV | NR | PFS |

Abbreviation: NR: not recorded; IQR: inter quantile range; std: standard deviation; IMRT: intensity modulated radiation therapy; IC: induction chemotherapy; AC: adjuvant chemotherapy; CCRT: concurrent chemoradiotherapy; RT: radiation therapy; CHT: chemotherapy; LRFS: Local Recurrence-Free Survival; DMFS: Distant Metastasis-Free Survival; PFS: Progression-Free Survival; DFS: Disease-Free Survival; FFS: Failure-Free Survival; OS: Overall Survival.

Table 2. MRI scanning details.

| Author | Slice Thickness | Tesla | Sequence | Scanner |
|-----------------------------------|-----------------|-----------------------------------|---|--|
| Khongwirotphan et al. (2024) [21] | 4 mm | 1.5 T | T1w, T2w | GE Signa HDxt |
| Qihao Zhang et al. (2023) [22] | 4 mm | 3 T | T1w, dynamic contrast-enhanced, Proton density | Siemens Skyra |
| Jiang Zhang et al. (2023) [23] | 3~4 mm | Train: 1.5 T/3 T; Test: 3 T | T1c | Train: Siemens Avanto; Test: GE SIGNA EXCITE, Siemens Avanto, Siemens Skyra, Philips Achieva |
| Li et al. (2023) [24] | 4 mm | 3 T | proton density-weighted, dynamic contrast-enhanced, T1c | Siemens Skyr |
| Hu et al. (2023) [25] | 4~6 mm | Train: 1.5 T/3 T; Test: 1.5 T/3 T | T1w, T2w, T1c | Train: GE Signa CV/I, Siemens Magnetom Tim Trio; Test: GE Signa Excite 1.5T HD Twin Speed, Philips Achieva 3.0T, Philips Intera 3.0T |
| Shen et al. (2022) [26] | NR | NR | T1w, T1c | NR |
| Liu et al. (2022) [27] | 4~5 mm | 3 T | T1w, T2w, T1c | Siemens MAGNETOM Verio |
| Li et al. (2022) [28] | 5 mm | 1.5 T/3 T | T1w, T2w, T1c | GE Signa CV/I; Siemens Magnetom Tim Trio |
| Jiang et al. (2022) [29] | 6 mm | 1.5 T | T1w, T2w, T1c | GE Signa EXCITE |
| Gao et al. (2021) [30] | 3 mm | 1.5 T | T1c | SIEMENS |
| Zhang et al. (2020) [31] | 3~5 mm | 1.5 T/3 T | T1w, T2wFS, T1cFS | Train: MAGNETOM Verio; Test: MAGNETOM Verio, Siemens Avanto |
| Bologna et al. (2020) [32] | NR | 1.5 T | T1w, T2w | |
| Zhang et al. (2019) [33] | 5~6 mm | 1.5 T | T1w, T2w, T1c | Train: GE Signa EXCITE, GE Signa HDx, SIEMENS Espree; Test: SIEMENS Novus15 |
| Ming et al. (2019) [34] | 6 mm | 1.5 T | T1c | GE Signa |
| Zhang et al. (2017) [35] | 4 mm | 1.5 T | T2, T1c | GE Signa EXCITE HD |

Abbreviation: NR: Not recorded; FS: Fat suppression.

Table 3. Summary of details of and prognosis model.

| Author | Segmentation Software | Annotator | Radiomics Software | Feature Selection | Feature Count | Radiomics Feature | Model | Result |
|-----------------------------------|---|-----------------------|---|--|-------------------------|---|-------------------------|------------------------------------|
| Khongwirotphan et al. (2024) [21] | Eclipse software https://journals.plos.org/plosone/article?id=10.1371/journal.pone.0298111 accessed on 23 April 2024 | Radiation oncologists | Pyradiomics v4.11 | interobserver variability test, univariate analysis with recursive feature elimination | OS: 9; PFS: 1; DMFS: 10 | OS: T2_original_shape_MinorAxisLength; T2_wavelet_HLH_glszm_LargeAreaEmphasis; T1_wavelet_LHL_firstorder_Energy; T1_original_shape_Sphericity; T1_wavelet_LLH_glcm_MaxiumProbability; T2_wavelt_LHL_ngtdm_Coarseness; T2_wavelet_LHL_firstorder_Median; T2_wavelet_LHL_gldtm_DependenceNonUniformity; T2_wavelet_HLL_gldm_DependenceNonUniformity; PFS: T2_wavelet_LHL_ngtdm_coarseness; DMFS: T1_original_shape_sphericity; T2_original_shape_Maxium3DDiameter; T2_wavelet_LHH_LargeAreaEmpasis; T2_wavelet_LHH_glszm_ZoneVariance; T1_original_shape_Maxium3DDiameter; T2_wavelet_LHL_ngtdm_Coarness; T2_wavelet_HHL_ngtdm_Coarness; T1_wavelet_LHL_gldm_DependenceNonUniformity; T1_original_glszm_ZoneEntropy; T1_wavelet_HLH_glszm_LargeAreaGrayLevelEmphasis | Cox proportional hazard | OS: 0.796; PFS: 0.708; DMFS: 0.766 |
| Qihao Zhang et al. (2023) [22] | ITK-SNAP v3.4.0 | Radiologist | Pyradiomics https://onlinelibrary.wiley.com/doi/10.1111/cas.15704 accessed on 23 April 2024 | LASSO | 19 | NonUniformity_PrecontrastDCE; SmallAreaEmphasis_PrecontrastDCE; Correlation_PostcontrastDCE (10 s); Minimum_PostcontrastDCE (15 s); 90Percentile_PostcontrastDCE (20 s); DifferenceVariance_PostcontrastDCE (20 s); LowGrayLevelZoneEmphasis_PostcontrastDCE (20 s); Autocorrelation_PostcontrastDCE (25 s); InverseVariance_PostcontrastDCE (25 s); HighGrayLevelEmphasis_PostcontrastDCE (25 s); SmallDependenceEmphasis_PostcontrastDCE (25 s); | Cox proportional hazard | PFS: 0.66 |

Table 3. Cont.

| Author | Segmentation Software | Annotator | Radiomics Software | Feature Selection | Feature Count | Radiomics Feature | Model | Result |
|--------------------------------|---|---------------------------|---|---|---------------|--|-------------------------|--|
| | | | | | | ShortRunHighGrayLevelEmphasis_PostcontrastDCE (25 s); LowGrayLevelZoneEmphasis_PostcontrastDCE (215 s); ClusterShade_PostcontrastDCE (220 s); ClusterShade_PostcontrastDCE (220 s); 90Percentile_T1Map; Median_T1Map; 90Percentile_ProtonDensityMap; Uniformity_ProtonDensityMap | | |
| Jiang Zhang et al. (2023) [23] | Eclipse Aria v13 | Treatment planning system | Pyradiomics v2.2.0 | volume dependency, ICC values, feature redundancy, outcome relevancy test | 10 | log.sigma.5.0.mm.3D_glszm_GrayLevelNonUniformity; wavelet.HLH_glszm_ZoneEntropy; wavelet.HLL_glszm_ZoneEntropy; wavelet.LLH_glszm_ZoneEntropy; original_shape_Sphericity; log.sigma.4.0.mm.3D_gldm_DependenceEntropy; wavelet.HHH_glrmlm_LowGrayLevelRunEmphasis; log.sigma.5.0.mm.3D_gldm_LowGrayLevelEmphasis; original_firstorder_Kurtosis; log.sigma.2.0.mm.3D_glrmlm_RunEntropy | Cox proportional hazard | DFS: 0.63 |
| Li et al. (2023) [24] | ITK-SNAP v3.6.0 | Radiologist | Pyradiomics v3.0.1 | Pearson correlation analysis, LASSO, backward feature elimination | 8 | PDw_wavelet-LHL_glszm_LAHGLE; PDw_lbp_firstorder_Variance from; T1c_wavelet-HHH_glszm_LAHGLE; T1c_squareroot_firstorder_RMAD; Ktrans_maximal correlation coefficient; Ktrans_gray level non-uniformity normalized; Kep_complexity; Kep_large dependence high gray level emphasis | Cox proportional hazard | PFS: 0.808 |
| Hu et al. (2023) [25] | 3D-Slicer v4.9.0 | Oncologist, Radiologist | Pyradiomics v2.1.2 | Pearson correlation, LASSO | 23 | NR | Cox proportional hazard | DMFS: 0.71 |
| Shen et al. (2022) [26] | in-house software https://www.sciencedirect.com/science/article/pii/S0167814022002225 accessed on 23 April 2024 | Radiologist | in-house software https://www.sciencedirect.com/science/article/pii/S0167814022002225 accessed on 23 April 2024 | intraclass correlation coefficients, univariate analysis, Pearson correlation coefficient, Boruta | 4 | NR | Cox proportional hazard | PFS: 0.726/0.691/0.723/0.704; LRRFS: 0.691/0.698/0.678/0.684; DMFS: 0.721/0.686/0.736/0.696; OS: 0.723/0.708/0.685/0.735 |

Table 3. Cont.

| Author | Segmentation Software | Annotator | Radiomics Software | Feature Selection | Feature Count | Radiomics Feature | Model | Result |
|------------------------|--|-------------|---|--|---------------|--|-------------------------|-------------|
| Liu et al. (2022) [27] | AccuContour software v3.0 | Radiologist | Pyradiomics https://www.ncbi.nlm.nih.gov/pmc/articles/PMC9021720/ accessed on 23 April 2024 | LASSO | 12 | T1.original.shape.Maximum2DDiameterRow; T1.wavelet.LLH.glcM.SumAverage; T1.wavelet.LHL.glcM.JointAverage; T1C.original.shape.MeshVolume; T1C.wavelet.LHL.firstorder.Median, T1C.wavelet.HLL.glcM.InverseVariance; T1C.wavelet.HLH.glszm. LargeAreaLowGrayLevelEmphasis; T2.wavelet.LLH.ngtdm.Coarseness; T2.wavelet.LHL.glcM.InverseVariance; T2.wavelet.LHL.glcM.MaximumProbability; T2.wavelet.LHH.firstorder.Maximum, T2.wavelet.HHL.glcM.MaximumProbability | Cox proportional hazard | OS: 0.807 |
| Li et al. (2022) [28] | AnalyzePro https://www.ncbi.nlm.nih.gov/pmc/articles/PMC8983880/ accessed on 23 April 2024 | Radiologist | Pyradiomics https://www.ncbi.nlm.nih.gov/pmc/articles/PMC8983880/ accessed on 23 April 2024 | interclass correlation coefficient, Pearson correlation coefficient, LASSO | 21 | T1_shape_Sphericity; T1_WLHH_GLSZM_LGLZE; T1_WHHL_GLCM_IMC2; T1_WHHH_GLCM_IMC2; T1_WHLH_GLCM_IMC2; T1_log.sigma.3.0.mm.3D_NGTDm_Strength; T1_WHHH_NGTDm_Contrast; T2_WHLL_GLDM_LDHGLE; T2_log.sigma.5.0.mm.3D_FOS_Skewness; T2_WHHL_GLSZM_SALGLE; T2_logarithm_NGTDm_Coarseness; T2_WLLH_GLCM_IDMN; T1C_WHLL_GLCM_Correlation; T1C_WLLH_GLSZM_SAHGLE, T1C_Gradient_GLCM_IMC1, T1C_Square_GLCM_Correlation; T1C_Gradient_GLSZM_ZE; T1C_square_GLRLM_RE; T1C_log.sigma.3.0.mm.3D_GLSZM_ZE; T1C_WLHL_GLSZM_ZE; T1C_gradient_GLSZM_GLN | Cox proportional hazard | DMFS: 0.711 |

Table 3. Cont.

| Author | Segmentation Software | Annotator | Radiomics Software | Feature Selection | Feature Count | Radiomics Feature | Model | Result |
|--------------------------|--|-------------|---|---|---------------|--|-------------------------|-----------|
| Jiang et al. (2022) [29] | RadCloud Radiomics Cloud Platform https://bmcmimedimaging.biomedcentral.com/articles/10.1186/s12880-022-00902-6 accessed on 23 April 2024 | NR | Pyradiomics v2.2.0 | interclass correlation coefficient, LASSO | 5 | T2WI_wavelet.LLL_Glrlm_ShortRunHighGrayLevelEmphasis; T1WI_original_Gldm_DependenceVariance; CE-T1WI_original_Ngtdm_Busyness; CE-T1WI_squareroot_Firstorder_Variance; CE-T1WI_wavelet.LLH_Gldm_LargeDependenceLowGrayLevelEmphasis | Cox proportional hazard | OS: 0.788 |
| Gao et al. (2021) [30] | Matlab v2018b | Radiologist | Pyradiomics https://onlinelibrary.wiley.com/doi/10.1002/hed.26867 accessed on 23 April 2024 | LASSO | 24 | Original-GLCM-Inverse Variance; Original-GLRLM-LRLGLE; Wavelet-HLL-Firstorder-Skewness; Wavelet-HLL-GLCM-Idmn; Wavelet-HLL-GLCM_Imc1; Wavelet-LHL-GLRLM-LRLGLE; Wavelet-LHH-Firstorder-Total Energy; Wavelet-LHH-GLCM-Joint Energy; Wavelet-LHH-GLCM-Idn; Wavelet-LHH-GLCM-Imc1; Wavelet-LLH-Firstorder-Skewness; Wavelet-LLH-GLCM-Imc2; Wavelet-HLH-Firstorder-Kurtosis; Wavelet-HHH-Firstorder-Median; Wavelet-HHH-Firstorder-Total Energy; Wavelet-HHH-Firstorder-Kurtosis; Wavelet-HHH-GLCM-Difference Variance; Wavelet-HHH-GLCM-Idn; Wavelet-HHH-GLCM-Cluster Prominence; Wavelet-HHH-GLCM-LRLGLE; Wavelet-HHL-GLCM-Inverse Variance; Wavelet-HHL-GLCM-Imc1; Wavelet-LLL-GLCM-MCC; Wavelet-LLL-GLCM-Imc2 | Cox proportional hazard | PFS: 0.73 |

Table 3. Cont.

| Author | Segmentation Software | Annotator | Radiomics Software | Feature Selection | Feature Count | Radiomics Feature | Model | Result |
|----------------------------|--|-------------|---|---|---------------|--|-------------------------|------------------------------------|
| Zhang et al. (2020) [31] | ITK-SNAP software v2.2.0 | Radiologist | Pyradiomics https://www.ncbi.nlm.nih.gov/pmc/articles/PMC7739087/ accessed on 23 April 2024 | intra/inter-class correlation coefficient, univariate analysis, minimal redundancy maximum relevance, and random forest | 12 | T1w_original_shape_LeastAxisLength; T1w_wavelet.HL_firstorder_Skewness; T2w_log.sigma.2.0.mm.3D_glcml_ClusterShade; T2w_wavelet.HL_glszm_SizeZoneNonUniformityNormalized; T2w_wavelet.HH_glcml_ClusterShade; T2w_original_glszm_SmallAreaLowGrayLevelEmphasis; T2w_log.sigma.3.0.mm.3D_glrml_LowGrayLevelRunEmphasis; T1c_wavelet.HH_glrml_LongRunLowGrayLevelEmphasis; T1c_wavelet.HH_glrml_ShortRunLowGrayLevelEmphasis; T1c_log.sigma.5.0.mm.3D_glcml_ClusterShade; T1c_wavelet.LH_glcml_Autocorrelation; T1c_wavelet.HH_firstorder_Skewness | Cox proportional hazard | FFS: 0.711 |
| Bologna et al. (2020) [32] | NR | Radiologist | Pyradiomics v2.2.0 | ICC, Spearman correlation coefficient, univariate and multivariate Cox regression | 2 | T-T1w-WaveletLLH-Firstorder-Median; T-T1w-WaveletLLL-Firstorder-Mean | Cox proportional hazard | OS: 0.68; DFS: 0.54; LRFS: 0.72 |
| Zhang et al. (2019) [33] | RadiAnt software https://www.ncbi.nlm.nih.gov/pmc/articles/PMC6491646/ accessed on 23 April 2024 | Radiologist | Matlab v2016a | recursive feature elimination, univariate and multivariate analysis | 11 | T2-w_GLCM_Cluster_S_Offset_8_Direction_135; T1-w_GLRLM_SRHGE_Direction_90; T1-w_IntensityDirect_Local_Entropy_Mean; T1-w_GLCM_Inverse_Variance_Offset_2_Direction_45; T1-w_GLCM_Contrast_Offset_4_Direction_90; T1-w_GLCM_Dissimilarity_Offset_4_Direction_90; subtraction_GLCM_Inverse_Variance_Offset_4_Direction_135; subtraction_GLCM_IMC_Offset_2_Direction_90; subtraction_IntensityHistogram_Quantile30; subtraction_NeighborIntensityDifference_Busyness; subtraction_GLCM_Cluster_P_Offset_8_Direction_90 | Cox proportional hazard | LRFS: 0.753 |

Table 3. Cont.

| Author | Segmentation Software | Annotator | Radiomics Software | Feature Selection | Feature Count | Radiomics Feature | Model | Result |
|--------------------------|--|-------------|--------------------|--|------------------------|---|-------------------------|-----------------------------------|
| Ming et al. (2019) [34] | MIM v6.6 | Oncologist | Matlab v2015a | Contour reproducibility and nonredundancy, LASSO | DFS: 5; OS: 3; DMFS: 4 | DFS:LL_GLCM.Information_Measures_II; HL_GLCM.Information_Measures_II; LL_HIST.mean; LL_HIST.kurtosis; HH_HIST.median; OS: HL_GLCM.Information_Measures_II; LL_HIST.skewness; LL_HIST.kurtosis; DMFS: LL_GLCM.Information_Measures_II; HL_GLCM.Information_Measures_II; LL_HIST.skewness; LL_HIST.kurtosis | Cox proportional hazard | DFS:0.674; OS: 0.694; DMFS: 0.669 |
| Zhang et al. (2017) [35] | ITK-SNAP https://aacrjournals.org/clincancerres/article/23/15/4259/257519/Radiomics-Features-of-Multiparametric-MRI-as-Novel accessed on 23 April 2024 | Radiologist | Matlab v2014a | LASSO | 7 | CET1-w_5_fos_mean; CET1-w_5_GLCM_correlation; CET1-w_5_GLRLM_RP; T2-w_Max3D; T2-w_3_fos_mean; T2-w_6_GLCM_IMC1; T2-w_1_GLRLM_SRLGLE | Cox proportional hazard | PFS: 0.758 |

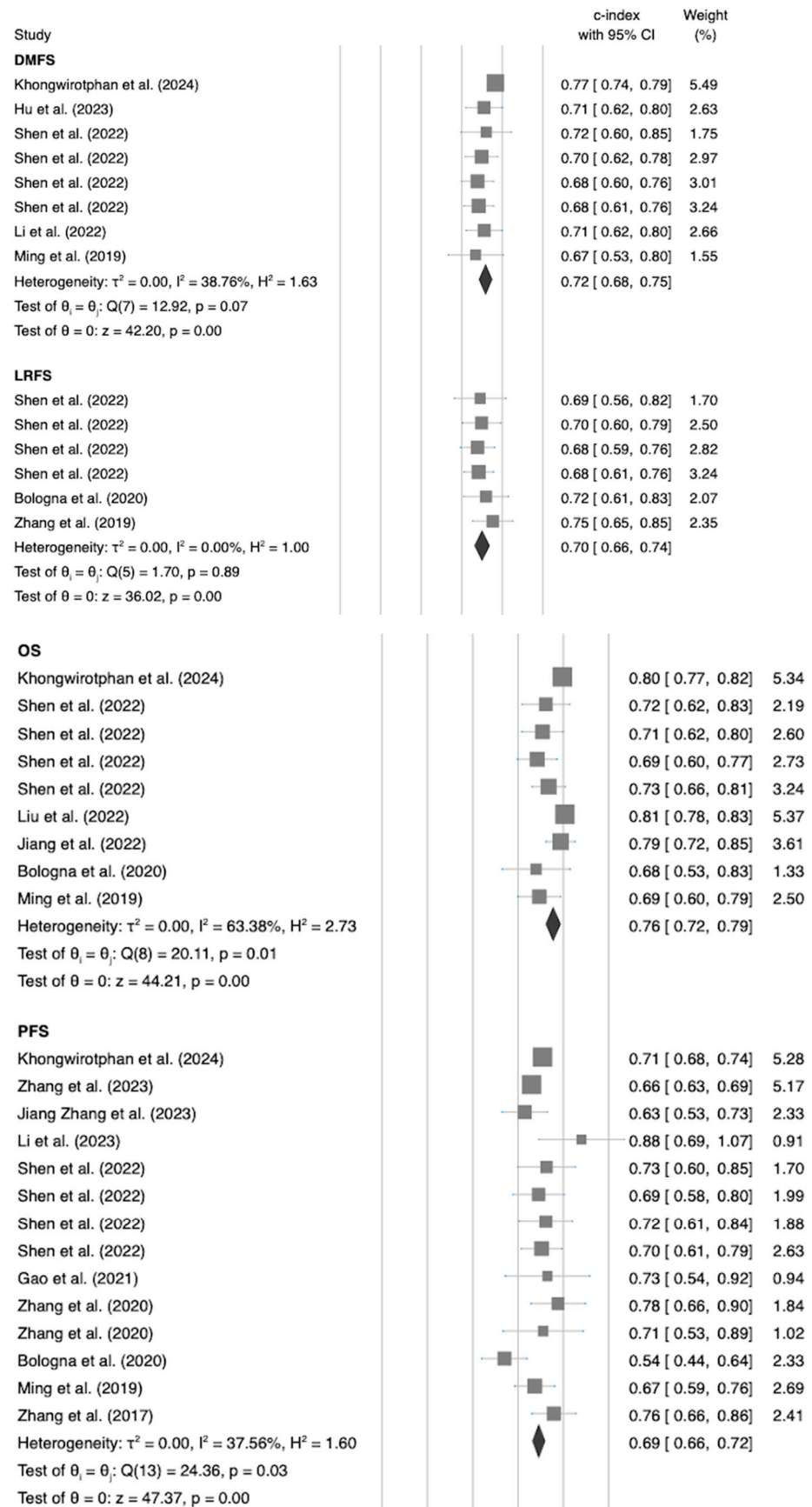


Figure 3. Forest plot of subgroup analysis of radiomics prognosis models' c-indexes with endpoint as moderator [21–35].

For Distant Metastasis-Free Survival (DMFS), we noted a c-index of 0.72 (95% CI: 0.68–0.75), with low variability ($I^2 = 38.76\%$). Local Recurrence-Free Survival (LRFS) demonstrated a c-index of 0.70 (95% CI: 0.66–0.74, $p = 0.89$) and showed no heterogeneity ($I^2 = 0\%$). Progression-Free Survival (PFS) had a c-index of 0.69 (95% CI: 0.66–0.72), with low heterogeneity ($I^2 = 37.56\%$). Lastly, Overall Survival (OS) presented a c-index of 0.76 (95% CI: 0.72–0.79), with moderate heterogeneity ($I^2 = 63.38\%$). These findings highlight the variability in the consistency of radiomics prognostic models across different oncological endpoints.

3.5. Secondary Outcome: Overall Survival Prediction of Radiomics Prognosis Model

Given that Overall Survival (OS) was the only endpoint associated with moderate heterogeneity, we conducted further subgroup analyses and meta-regression to identify potential moderators that could explain this heterogeneity. Significant differences were observed when considering the validation method and radiomics software as moderators (see Table 4). Specifically, subgroups based on radiomics software exhibited low heterogeneity, although caution is advised due to potential bias from the small number of studies included [131]. This observation warrants confirmation with additional studies.

Table 4. Subgroup analysis of radiomics prognosis model with Overall Survival as endpoint.

| Moderator | N of Studies | c-Index (95% CI) | p-Values | % I^2 |
|--------------------|--------------|------------------|----------|---------|
| Region | | | 0.33 | |
| Asian | 8 | 0.76 (0.72~0.79) | <0.01 | 70% |
| Europe | 1 | 0.68 (0.53~0.83) | <0.01 | 0% |
| Validation method | | | 0.03 | |
| External | 3 | 0.71 (0.67~0.76) | <0.01 | 0% |
| Internal | 6 | 0.78 (0.74~0.81) | <0.01 | 56% |
| MRI sequence | | | 0.20 | |
| Multiple | 8 | 0.76 (0.72~0.80) | <0.01 | 67% |
| Single | 1 | 0.69 (0.60~0.79) | <0.01 | 0% |
| Radiomics software | | | <0.01 | |
| In-house | 5 | 0.71 (0.67~0.75) | <0.01 | 1% |
| Pyradiomics | 4 | 0.80 (0.72~0.79) | <0.01 | 3% |

In our meta-regression analysis, a significant association ($p < 0.01$) was found between the number of features in the prognosis model and its performance, with a coefficient of 0.010622 (Figure 4). No significant association was found with the publication year (coefficient = 0.0220509, $p = 0.084$). There was also no significant relationship between training size (coefficient = 2.72×10^{-6} , $p = 0.985$) and model performance.

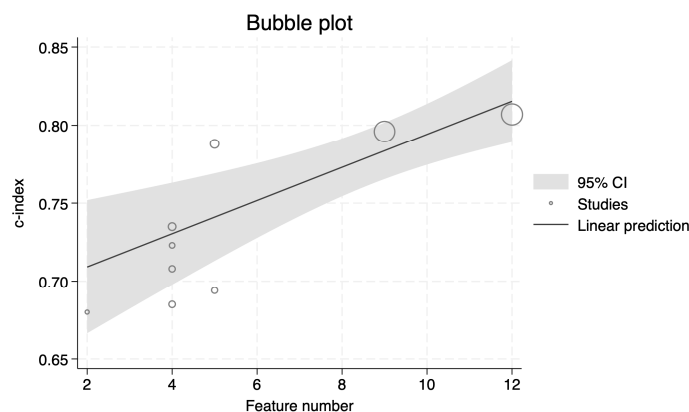


Figure 4. Bubble plot of feature number on radiomics prognosis models with Overall Survival as endpoint.

4. Discussion

4.1. Overview of Key Findings

Our meta-analysis systematically evaluated 37 radiomics prognostic outcomes, revealing a notable average concordance index (c-index) of 72% (95% Confidence Interval (CI): 70–74%) across studies, with the range stretching from 54% to 81%. This variation not only underscores the potential utility of radiomics in clinical prognostication but also highlights the substantial heterogeneity encountered, particularly in Overall Survival (OS) predictions, where a moderate Higgins I^2 statistic of 64.44% was observed. Notably, our findings identified a significant positive correlation between the number of features in the prognosis model and its performance, with a meta-regression coefficient of 0.010622 ($p < 0.01$), emphasizing the complexity and potential of detailed models. The analysis also demonstrated that validation methods and radiomics software significantly influenced heterogeneity, pinpointing crucial areas for standardization and improvement in future research.

4.2. Comparison with Existing Literature

When compared with the existing literature, our findings both validate the recognized potential of radiomics and highlight the challenges of achieving consistent performance across studies. Notably, the c-index range we report aligns with those found in similar meta-analyses, such as a c-index of 0.762 (95% CI, 0.687–0.837) for Progression-Free Survival (PFS) prediction [13]. Similarly, we limited our analysis to prognosis models incorporating radiomics features. However, we further refined our approach by categorizing endpoints into more sophisticated subgroups, leading to observed reductions in heterogeneity for Local Recurrence-Free Survival (LRFS), Distant Metastasis-Free Survival (DMFS), and PFS. Additionally, our study aggregated results for Overall Survival (OS), an analysis not conducted in the prior study. The moderate heterogeneity observed in OS predictions ($I^2 = 64.44\%$) suggests that OS may be influenced by a broader range of clinical conditions, potentially necessitating the inclusion of additional clinical features for more robust prediction models.

Our analysis also advances the discussion on methodological variables—specifically, the number of features in a model and the selection of radiomics software. These factors have been less frequently quantified in prior reviews. By highlighting these aspects, our study underscores the need for a more standardized approach to radiomics model development, potentially leading to more consistent and reliable prognostic tools.

4.3. Implications for Clinical Practice and Research

The significance of our findings is emphasized through the substantial average concordance index, indicating that radiomic models harbor the potential to considerably refine patient stratification and the planning of treatments. Nonetheless, the observed diversity and fluctuations in performance, especially concerning Overall Survival (OS) predictions, mandate a prudent integration into clinical guidelines.

The observed variability in the consistency of radiomics prognostic models across different oncological endpoints has important implications for clinical practice. The finding that models performed more consistently for Local Recurrence-Free Survival (LRFS), Distant Metastasis-Free Survival (DMFS), and Progression-Free Survival (PFS) compared to OS suggests that radiomics may be particularly useful for predicting locoregional control and disease progression. This could help clinicians identify high-risk patients who may need more aggressive local therapies or closer surveillance. However, the greater variability in performance for OS indicates that radiomics alone may not be as reliable for predicting long-term survival, which is impacted by many factors beyond the primary tumor.

These results underscore the need to carefully consider the specific clinical endpoint of interest when developing and applying radiomics prognostic models. Models that perform well for one endpoint may not necessarily generalize to other endpoints. Clinicians should look for models that have been validated for the specific outcomes most relevant to their patients and practice. The variability across endpoints also highlights the importance of

incorporating other clinical, pathologic, and genomic factors alongside radiomics to develop more holistic prognostic models, particularly for OS. Radiomics can provide valuable information about the primary tumor, but integrating it with other key determinants of survival may be necessary to maximize prognostic value.

Crucially, our detailed subgroup analysis and meta-regression reveals distinct moderators (for instance, validation methodologies profoundly affecting heterogeneity and radiomic software that reduces subgroup heterogeneity) that, upon standardization, could streamline the enhancement and validation of radiomic models. This standardization is pivotal for augmenting their reliability and applicability within clinical frameworks, thus facilitating improved patient care and treatment outcomes.

Despite these promising avenues, moderate heterogeneity in OS predictions persists, highlighting the complex interplay between radiomic data and patient-specific clinical factors such as health status, comorbidities, and response to treatment. The multifactorial nature of OS suggests that while radiomics can provide valuable insights into tumor characteristics, a comprehensive approach that integrates radiomic data with clinical parameters is essential for making more accurate prognostic assessments. Moreover, variations in treatment protocols and intrinsic tumor heterogeneity contribute further to the observed disparities in survival predictions.

Finally, the results suggest that further research is needed to understand the biological underpinnings of the radiomics features that drive prognostic performance for different endpoints. Better mechanistic insight could help refine models and identify radiomics signatures that are more specifically linked to the most clinically meaningful outcomes. Ongoing research to refine and integrate radiomics into multifaceted prognostic models will be key to realizing its potential to guide precision oncology care.

4.4. Technical Considerations of Radiomics Features and Imaging Protocols

Standardized approaches have been implemented to address the potential risk of bias due to protocol variations in radiomics studies to ensure consistency and comparability across different cancer pathologies. Khanfari et al. [132] employed a standardized dataset alongside consistent preprocessing techniques, including normalization and enhancement across various mpMRI images. This method was vital for minimizing data handling variability and included the use of uniform fusion techniques and robust preprocessing methods, which are essential in prostate cancer grading and reducing bias from data processing variations. Similarly, Reginelli et al. [133] standardized the radiomics pipeline by using consistent image acquisition protocols and radiomics software, thus enhancing the reliability of their findings and mitigating the risk of bias across studies.

To further ensure the relevance and accuracy of prognosis models, statistical techniques and machine learning were used for selecting radiomics features. Methods like the Least Absolute Shrinkage and Selection Operator (LASSO), recursive feature elimination, and correlation analyses (Pearson and Spearman) identified features with minimal redundancy. The reproducibility and consistency of these features were evaluated using intraclass and interclass correlation coefficients. Univariate and multivariate analyses, including Cox regression, further refined the selection based on statistical significance and clinical relevance.

Additionally, robust radiomics software was utilized to normalize data across different MRI scanner settings, mitigating the impact of scanning variability on feature extraction and model performance. MRI sequences were categorized into single and multiple sequences to examine how sequence variations affect the predictive power of radiomics features. This structured approach clarified the influence of technical variations in MRI on radiomic analysis and enhanced the results' reliability and applicability. These comprehensive measures effectively addressed potential biases due to protocol variations, leading to more reliable and applicable outcomes in radiomics studies.

4.5. Methodological Considerations and Strengths

The foundational strength of our study lies in its methodological precision, highlighted by a meticulous systematic review and exhaustive analyses, including the use of meta-regression to identify sources of heterogeneity. The employment of established evaluation tools such as the Quality in Prognosis Studies (QUIPS) and the Radiomics Quality Score (RQS) enhances the reliability of our findings. QUIPS provides a qualitative assessment of bias across various domains of prognostic studies, adding depth to our analysis, while the RQS offers a quantitative measure of methodological quality. Higher RQS scores denote studies with lower risks of bias and greater methodological reliability, essential for ensuring the validity and reproducibility of results. This scoring system not only aids in distinguishing high-quality studies but also pinpoints areas needing improvement in study design and execution.

Moreover, the integration of RQS in a meta-regression against study results allows for a nuanced exploration of how methodological quality impacts reported outcomes in radiomics research. Our findings from the meta-regression, showing a coefficient of -0.0083655 with a p -value of 0.294 , indicate no significant association between RQS scores and study outcomes at conventional levels of statistical significance. This analysis underscores the importance of robust methodological design in influencing the findings of radiomics studies and provides a reproducible framework for future research in this evolving field.

4.6. Limitations and Future Research Directions

Notwithstanding the compelling nature of our results, they are accompanied by limitations. The marked heterogeneity ($I^2 = 64.44\%$ for OS), potential biases, and paucity of studies within certain subgroups reflect the intricate nature of radiomics research and might temper the strength of our deductions. The inability to include unpublished studies raises the possibility of publication bias, while heterogeneity in patient populations, treatments, endpoints, and radiomics methods may limit the reliability and generalizability of pooled estimates. The retrospective nature of the included studies, lack of prospective validation, and absence of a direct assessment of the clinical utility of radiomics compared to standard prognostic tools are also important limitations that underscore the need for ongoing research.

Future inquiries should focus on conducting multi-institutional prospective studies to validate radiomics models in diverse patient cohorts and real-world settings. Methodological standardization, integration of radiomics with other prognostic factors, and mechanistic investigations are key priorities. Rigorous assessments of the clinical utility and impact of integrating radiomics into prognostic models and treatment strategies are essential. Expanding radiomics research to other cancer types and imaging modalities, as well as fostering multidisciplinary collaboration and data sharing, will be crucial for advancing the field. Such endeavors are pivotal for bridging the gap between radiomics research and its clinical application, ultimately leading to more effective and personalized treatment approaches. By addressing these challenges and opportunities, future research can help transform radiomics from a promising research tool into a validated and impactful asset for advancing precision oncology.

5. Conclusions

In summary, our meta-analysis highlighted the significance and variability of radiomics in predicting cancer treatment outcomes, particularly focusing on overall survival due to its heterogeneity.

Supplementary Materials: The following supporting information can be downloaded at <https://www.mdpi.com/article/10.3390/diagnostics14090924/s1>. Figure S1: Sensitivity analysis of radiomics prognosis models' c-index with leave one out method. Figure S2: Funnel plot of radiomics prognosis models' c-index group by different endpoint. Table S1. PRISMA Checklist. Table S2. Keywords and

search results in different databases. Table S3. Excluded article and reason. Table S4. Details of QUIPS assessment. Table S5. Details of radiomic quality score.

Author Contributions: Conceptualization, C.-K.W., T.-W.W., C.-F.L., Y.-T.W. and M.-W.H.; methodology, C.-K.W. and T.-W.W.; software, T.-W.W.; validation, C.-K.W. and T.-W.W.; formal analysis, C.-K.W. and T.-W.W.; investigation, C.-K.W. and T.-W.W.; resources, Y.-T.W. and M.-W.H.; data curation, C.-K.W. and T.-W.W.; writing—original draft preparation, C.-K.W. and T.-W.W.; writing—review and editing, C.-K.W., T.-W.W., C.-F.L., Y.-T.W. and M.-W.H.; visualization, T.-W.W.; supervision, Y.-T.W. and M.-W.H.; project administration, Y.-T.W. and M.-W.H.; funding acquisition, M.-W.H. All authors have read and agreed to the published version of the manuscript.

Funding: This research was funded by the Gen. & Mrs. M.C. Peng Fellowship from School of Medicine, National Yang Ming Chiao Tung University, MD-SY-A3-309-01, MD-SY-A3-112-C3-08, MD-SY-112-C3-09, MD-SY-112-C3-010 and MD-SY-112-C3-011.

Institutional Review Board Statement: This meta-analysis did not intervene or interact with humans or collect identifiable private information and, thus, does not require institutional review board approval.

Informed Consent Statement: Not applicable.

Data Availability Statement: Data are contained within the article and Supplementary Files.

Conflicts of Interest: The authors declare no conflicts of interest.

References

1. Chua, M.L.K.; Wee, J.T.S.; Hui, E.P.; Chan, A.T.C. Nasopharyngeal carcinoma. *Lancet* **2016**, *387*, 1012–1024. [[CrossRef](#)] [[PubMed](#)]
2. Wei, W.I.; Sham, J.S. Nasopharyngeal carcinoma. *Lancet* **2005**, *365*, 2041–2054. [[CrossRef](#)] [[PubMed](#)]
3. Lambin, P.; Rios-Velazquez, E.; Leijenaar, R.; Carvalho, S.; van Stiphout, R.G.P.M.; Granton, P.; Zegers, C.M.L.; Gillies, R.; Boellard, R.; Dekker, A.; et al. Radiomics: Extracting more information from medical images using advanced feature analysis. *Eur. J. Cancer* **2012**, *48*, 441–446. [[CrossRef](#)] [[PubMed](#)]
4. Aerts, H.J.; Velazquez, E.R.; Leijenaar, R.T.; Parmar, C.; Grossmann, P.; Carvalho, S.; Bussink, J.; Monshouwer, R.; Haibe-Kains, B.; Rietveld, D.; et al. Decoding tumour phenotype by noninvasive imaging using a quantitative radiomics approach. *Nat. Commun.* **2014**, *5*, 4006. [[CrossRef](#)] [[PubMed](#)]
5. Gillies, R.J.; Kinahan, P.E.; Hricak, H. Radiomics: Images Are More than Pictures, They Are Data. *Radiology* **2016**, *278*, 563–577. [[CrossRef](#)]
6. Kumar, V.; Gu, Y.; Basu, S.; Berglund, A.; Eschrich, S.A.; Schabath, M.B.; Forster, K.; Aerts, H.J.W.L.; Dekker, A.; Fenstermacher, D.; et al. Radiomics: The process and the challenges. *Magn. Reson. Imaging* **2012**, *30*, 1234–1248. [[CrossRef](#)] [[PubMed](#)]
7. Leijenaar, R.T.H.; Carvalho, S.; Hoebens, F.J.P.; Aerts, H.J.W.L.; van Elmpt, W.J.C.; Huang, S.H.; Chan, B.; Waldron, J.N.; O’Sullivan, B.; Lambin, P. External validation of a prognostic CT-based radiomic signature in oropharyngeal squamous cell carcinoma. *Acta Oncol.* **2015**, *54*, 1423–1429. [[CrossRef](#)] [[PubMed](#)]
8. Zhang, B.; He, X.; Ouyang, F.; Gu, D.; Dong, Y.; Zhang, L.; Mo, X.; Huang, W.; Tian, J.; Zhang, S. Radiomic machine-learning classifiers for prognostic biomarkers of advanced nasopharyngeal carcinoma. *Cancer Lett.* **2017**, *403*, 21–27. [[CrossRef](#)]
9. Huang, Y.-Q.; Liang, C.-H.; He, L.; Tian, J.; Liang, C.-S.; Chen, X.; Ma, Z.-L.; Liu, Z.-Y. Development and Validation of a Radiomics Nomogram for Preoperative Prediction of Lymph Node Metastasis in Colorectal Cancer. *J. Clin. Oncol.* **2016**, *34*, 2157–2164. [[CrossRef](#)]
10. Ouyang, F.-S.; Guo, B.-L.; Zhang, B.; Dong, Y.-H.; Zhang, L.; Mo, X.-K.; Huang, W.-H.; Zhang, S.-X.; Hu, Q.-G. Exploration and validation of radiomics signature as an independent prognostic biomarker in stage III-IVb nasopharyngeal carcinoma. *Oncotarget* **2017**, *8*, 74869–74879. [[CrossRef](#)]
11. Wang, T.-W.; Chao, H.-S.; Chiu, H.-Y.; Lin, Y.-H.; Chen, H.-C.; Lu, C.-F.; Liao, C.-Y.; Lee, Y.; Shiao, T.-H.; Chen, Y.-M.; et al. Evaluating the Potential of Delta Radiomics for Assessing Tyrosine Kinase Inhibitor Treatment Response in Non-Small Cell Lung Cancer Patients. *Cancers* **2023**, *15*, 5125. [[CrossRef](#)] [[PubMed](#)]
12. Wang, T.-W.; Chao, H.-S.; Chiu, H.-Y.; Lu, C.-F.; Liao, C.-Y.; Lee, Y.; Chen, J.-R.; Shiao, T.-H.; Chen, Y.-M.; Wu, Y.-T. Radiomics of metastatic brain tumor as a predictive image biomarker of progression-free survival in patients with non-small-cell lung cancer with brain metastasis receiving tyrosine kinase inhibitors. *Transl. Oncol.* **2024**, *39*, 101826. [[CrossRef](#)] [[PubMed](#)]
13. Lee, S.; Choi, Y.; Seo, M.-K.; Jang, J.; Shin, N.-Y.; Ahn, K.-J.; Kim, B.-S. Magnetic Resonance Imaging-Based Radiomics for the Prediction of Progression-Free Survival in Patients with Nasopharyngeal Carcinoma: A Systematic Review and Meta-Analysis. *Cancers* **2022**, *14*, 653. [[CrossRef](#)] [[PubMed](#)]
14. Page, M.J.; McKenzie, J.E.; Bossuyt, P.M.; Boutron, I.; Hoffmann, T.C.; Mulrow, C.D. The PRISMA 2020 statement: An updated guideline for reporting systematic reviews Systematic reviews and Meta-Analyses. *BMJ* **2021**, *372*, 71. [[CrossRef](#)]
15. Mayr, A.; Schmid, M. Boosting the concordance index for survival data—A unified framework to derive and evaluate biomarker combinations. *PLoS ONE* **2014**, *9*, e84483. [[CrossRef](#)]

16. Hayden, J.A.; Van Der Windt, D.A.; Cartwright, J.L.; Côté, P.; Bombardier, C. Assessing bias in studies of prognostic factors. *Ann. Intern. Med.* **2013**, *158*, 280–286. [[CrossRef](#)]
17. Lambin, P.; Leijenaar, R.T.H.; Deist, T.M.; Peerlings, J.; de Jong, E.E.C.; van Timmeren, J.; Sanduleanu, S.; Larue, R.T.H.M.; Even, A.J.G.; Jochems, A.; et al. Radiomics: The bridge between medical imaging and personalized medicine. *Nat. Rev. Clin. Oncol.* **2017**, *14*, 749–762. [[CrossRef](#)]
18. Borenstein, M.; Hedges, L.V.; Rothstein, H.R. Fixed-Effect versus Random-Effects Models. In *Introduction to Meta-Analysis*; Borenstein, M., Ed.; Wiley: Hoboken, NJ, USA, 2009; pp. 77–86.
19. Higgins, J.P.T.; Thompson, S.G.; Deeks, J.J.; Altman, D.G. Measuring Inconsistency in Meta-Analyses. *BMJ* **2003**, *327*, 557–560. [[CrossRef](#)]
20. Egger, M.; Smith, G.D.; Schneider, M.; Minder, C. Bias in Meta-Analysis Detected by a Simple, Graphical Test. *BMJ* **1997**, *315*, 629–634. [[CrossRef](#)]
21. Khongwirotpahan, S.; Oonsiri, S.; Kitpanit, S.; Prayongrat, A.; Kannarunimit, D.; Chakkabat, C.; Lertbutsayanukul, C.; Sriswasdi, S.; Rakvongthai, Y. Multimodality radiomics for tumor prognosis in nasopharyngeal carcinoma. *PLoS ONE* **2024**, *19*, e0298111. [[CrossRef](#)]
22. Zhang, Q.; Wu, G.; Yang, Q.; Dai, G.; Li, T.; Chen, P.; Li, J.; Huang, W. Survival rate prediction of nasopharyngeal carcinoma patients based on MRI and gene expression using a deep neural network. *Cancer Sci.* **2023**, *114*, 1596–1605. [[CrossRef](#)] [[PubMed](#)]
23. Zhang, J.; Lam, S.-K.; Teng, X.; Ma, Z.; Han, X.; Zhang, Y.; Cheung, A.L.-Y.; Chau, T.-C.; Ng, S.C.-Y.; Lee, F.K.-H.; et al. Radiomic feature repeatability and its impact on prognostic model generalizability: A multi-institutional study on nasopharyngeal carcinoma patients. *Radiother. Oncol.* **2023**, *183*, 109578. [[CrossRef](#)] [[PubMed](#)]
24. Li, H.; Huang, W.; Wang, S.; Balasubramanian, P.S.; Wu, G.; Fang, M.; Xie, X.; Zhang, J.; Dong, D.; Tian, J.; et al. Comprehensive integrated analysis of MR and DCE-MR radiomics models for prognostic prediction in nasopharyngeal carcinoma. *Vis. Comput. Ind. Biomed. Art* **2023**, *6*, 23. [[CrossRef](#)] [[PubMed](#)]
25. Hu, Y.-J.; Zhang, L.; Xiao, Y.-P.; Lu, T.-Z.; Guo, Q.-J.; Lin, S.-J.; Liu, L.; Chen, Y.-B.; Huang, Z.-L.; Liu, Y.; et al. MRI-based deep learning model predicts distant metastasis and chemotherapy benefit in stage II nasopharyngeal carcinoma. *iScience* **2023**, *26*, 106932. [[CrossRef](#)] [[PubMed](#)]
26. Shen, H.; Yin, J.; Niu, R.; Lian, Y.; Huang, Y.; Tu, C.; Liu, D.; Wang, X.; Lan, X.; Yuan, X.; et al. MRI-based radiomics to compare the survival benefit of induction chemotherapy plus concurrent chemoradiotherapy versus concurrent chemoradiotherapy plus adjuvant chemotherapy in locoregionally advanced nasopharyngeal carcinoma: A multicenter study. *Radiother. Oncol.* **2022**, *171*, 107–113. [[CrossRef](#)] [[PubMed](#)]
27. Liu, K.; Qiu, Q.; Qin, Y.; Chen, T.; Zhang, D.; Huang, L.; Yin, Y.; Wang, R. Radiomics Nomogram Based on Multiple-Sequence Magnetic Resonance Imaging Predicts Long-Term Survival in Patients Diagnosed With Nasopharyngeal Carcinoma. *Front. Oncol.* **2022**, *12*, 852348. [[CrossRef](#)] [[PubMed](#)]
28. Li, H.-J.; Liu, L.-Z.; Huang, Y.; Jin, Y.-B.; Chen, X.-P.; Luo, W.; Su, J.-C.; Chen, K.; Zhang, J.; Zhang, G.-Y. Establishment and Validation of a Novel MRI Radiomics Feature-Based Prognostic Model to Predict Distant Metastasis in Endemic Nasopharyngeal Carcinoma. *Front. Oncol.* **2022**, *12*, 794975. [[CrossRef](#)]
29. Jiang, S.; Han, L.; Liang, L.; Long, L. Development and validation of an MRI-based radiomic model for predicting overall survival in nasopharyngeal carcinoma patients with local residual tumors after intensity-modulated radiotherapy. *BMC Med. Imaging* **2022**, *22*, 174. [[CrossRef](#)] [[PubMed](#)]
30. Gao, Y.; Mao, Y.; Lu, S.; Tan, L.; Li, G.; Chen, J.; Huang, D.; Zhang, X.; Qiu, Y.; Liu, Y. Magnetic resonance imaging-based radiogenomics analysis for predicting prognosis and gene expression profile in advanced nasopharyngeal carcinoma. *Head Neck* **2021**, *43*, 3730–3742. [[CrossRef](#)]
31. Zhang, F.; Zhong, L.-Z.; Zhao, X.; Dong, D.; Yao, J.-J.; Wang, S.-Y.; Liu, Y.; Zhu, D.; Wang, Y.; Wang, G.-J.; et al. A deep-learning-based prognostic nomogram integrating microscopic digital pathology and macroscopic magnetic resonance images in nasopharyngeal carcinoma: A multi-cohort study. *Ther. Adv. Med. Oncol.* **2020**, *12*, 1758835920971416. [[CrossRef](#)]
32. Bologna, M.; Corino, V.; Calareso, G.; Tenconi, C.; Alfieri, S.; Iacovelli, N.A.; Cavallo, A.; Cavalieri, S.; Locati, L.; Bossi, P.; et al. Baseline MRI-Radiomics Can Predict Overall Survival in Non-Endemic EBV-Related Nasopharyngeal Carcinoma Patients. *Cancers* **2020**, *12*, 2958. [[CrossRef](#)] [[PubMed](#)]
33. Zhang, L.-L.; Huang, M.-Y.; Li, Y.; Liang, J.-H.; Gao, T.-S.; Deng, B.; Yao, J.-J.; Lin, L.; Chen, F.-P.; Huang, X.-D.; et al. Pretreatment MRI radiomics analysis allows for reliable prediction of local recurrence in non-metastatic T4 nasopharyngeal carcinoma. *EBioMedicine* **2019**, *42*, 270–280. [[CrossRef](#)] [[PubMed](#)]
34. Ming, X.; Oei, R.W.; Zhai, R.; Kong, F.; Du, C.; Hu, C.; Hu, W.; Zhang, Z.; Ying, H.; Wang, J. MRI-based radiomics signature is a quantitative prognostic biomarker for nasopharyngeal carcinoma. *Sci. Rep.* **2019**, *9*, 10412. [[CrossRef](#)] [[PubMed](#)]
35. Zhang, B.; Tian, J.; Dong, D.; Gu, D.; Dong, Y.; Zhang, L.; Lian, Z.; Liu, J.; Luo, X.; Pei, S.; et al. Radiomics Features of Multiparametric MRI as Novel Prognostic Factors in Advanced Nasopharyngeal Carcinoma. *Clin. Cancer Res.* **2017**, *23*, 4259–4269. [[CrossRef](#)] [[PubMed](#)]
36. Xi, Y.; Dong, H.; Wang, M.; Chen, S.; Han, J.; Liu, M.; Jiang, F.; Ding, Z. Early prediction of long-term survival of patients with nasopharyngeal carcinoma by multi-parameter MRI radiomics. *Eur. J. Radiol. Open* **2024**, *12*, 100543. [[CrossRef](#)] [[PubMed](#)]
37. Sheng, J.; Lam, S.; Zhang, J.; Zhang, Y.; Cai, J. Multi-omics fusion with soft labeling for enhanced prediction of distant metastasis in nasopharyngeal carcinoma patients after radiotherapy. *Comput. Biol. Med.* **2024**, *168*, 107684. [[CrossRef](#)] [[PubMed](#)]

38. Ding, J.; Chen, J.; Lin, Y.; Hong, J.; Huang, C.; Fei, Z.; Chen, C. Significance of radiologic extranodal extension in locoregionally advanced nasopharyngeal carcinoma with lymph node metastasis: A comprehensive nomogram. *Braz. J. Otorhinolaryngol.* **2024**, *90*, 101363. [[CrossRef](#)] [[PubMed](#)]
39. Zhang, Y.; Ye, X.; Ge, J.; Guo, D.; Zheng, D.; Yu, H.; Chen, Y.; Yao, G.; Lu, Z.; Yuille, A.; et al. Deep Learning-Based Multi-Modality Segmentation of Primary Gross Tumor Volume in CT and MRI for Nasopharyngeal Carcinoma. *Int. J. Radiat. Oncol. Biol. Phys.* **2023**, *117*, e498. [[CrossRef](#)]
40. Zhang, B.; Luo, C.; Zhang, X.; Hou, J.; Liu, S.; Gao, M.; Zhang, L.; Jin, Z.; Chen, Q.; Yu, X.; et al. Integrative Scoring System for Survival Prediction in Patients With Locally Advanced Nasopharyngeal Carcinoma: A Retrospective Multicenter Study. *JCO Clin. Cancer Inform.* **2023**, *7*, e2200015. [[CrossRef](#)]
41. Yao, Y.; Sun, X.; Huang, H.; Wang, Z.; Fang, X.; Chen, M.; Chen, Z.; Weng, H.; Guo, C.; Hong, H.; et al. Proposed prognostic subgroups and facilitated clinical decision-making for additional locoregional radiotherapy in de novo metastatic nasopharyngeal carcinoma: A retrospective study based on recursive partitioning analysis. *Radiat. Oncol.* **2023**, *18*, 15. [[CrossRef](#)]
42. Yang, C.; Chen, Y.; Zhu, L.; Wang, L.; Lin, Q. A deep learning MRI-based signature may provide risk-stratification strategies for nasopharyngeal carcinoma. *Eur. Arch. Oto-Rhino-Laryngol.* **2023**, *280*, 5039–5047. [[CrossRef](#)] [[PubMed](#)]
43. Xu, H.; Wang, A.; Zhang, C.; Ren, J.; Zhou, P.; Liu, J. Intra- and peritumoral MRI radiomics assisted in predicting radiochemotherapy response in metastatic cervical lymph nodes of nasopharyngeal cancer. *BMC Med. Imaging* **2023**, *23*, 66. [[CrossRef](#)] [[PubMed](#)]
44. Xu, H.; Lv, W.; Zhang, H.; Yuan, Q.; Wang, Q.; Wu, Y.; Lu, L. Multimodality radiomics analysis based on [18F]FDG PET/CT imaging and multisequence MRI: Application to nasopharyngeal carcinoma prognosis. *Eur. Radiol.* **2023**, *33*, 6677–6688. [[CrossRef](#)] [[PubMed](#)]
45. Wu, Q.; Chang, Y.; Yang, C.; Liu, H.; Chen, F.; Dong, H.; Chen, C.; Luo, Q. Adjuvant chemotherapy or no adjuvant chemotherapy? A prediction model for the risk stratification of recurrence or metastasis of nasopharyngeal carcinoma combining MRI radiomics with clinical factors. *PLoS ONE* **2023**, *18*, e0287031. [[CrossRef](#)] [[PubMed](#)]
46. Wu, M.; Xu, W.; Fei, Y.; Li, Y.; Yuan, J.; Qiu, L.; Zhang, Y.; Chen, G.; Cheng, Y.; Cao, Y.; et al. MRI-based clinical radiomics nomogram may predict the early response after concurrent chemoradiotherapy in locally advanced nasopharyngeal carcinoma. *Front. Oncol.* **2023**, *13*, 1192953. [[CrossRef](#)]
47. Wang, S.; Yang, Y.; Xie, H.; Yang, X.; Liu, Z.; Li, H.; Huang, W.; Luo, W.; Lei, Y.; Sun, Y.; et al. Delta-Radiomics Guides Adaptive De-Intensification after Induction Chemotherapy in Locoregionally Advanced Nasopharyngeal Carcinoma in the IMRT Era. *Int. J. Radiat. Oncol. Biol. Phys.* **2023**, *117*, S152–S153. [[CrossRef](#)]
48. Wang, A.; Xu, H.; Zhang, C.; Ren, J.; Liu, J.; Zhou, P. Radiomic analysis of MRI for prediction of response to induction chemotherapy in nasopharyngeal carcinoma patients. *Clin. Radiol.* **2023**, *78*, e644–e653. [[CrossRef](#)] [[PubMed](#)]
49. Teng, X.; Zhang, J.; Han, X.; Sun, J.; Lam, S.-K.; Ai, Q.-Y.H.; Ma, Z.; Lee, F.K.-H.; Au, K.-H.; Yip, C.W.-Y.; et al. Explainable machine learning via intra-tumoral radiomics feature mapping for patient stratification in adjuvant chemotherapy for locoregionally advanced nasopharyngeal carcinoma. *La Radiol. Med.* **2023**, *128*, 828–838. [[CrossRef](#)]
50. Sun, M.-X.; Zhao, M.-J.; Zhao, L.-H.; Jiang, H.-R.; Duan, Y.-X.; Li, G. A nomogram model based on pre-treatment and post-treatment MR imaging radiomics signatures: Application to predict progression-free survival for nasopharyngeal carcinoma. *Radiat. Oncol.* **2023**, *18*, 67. [[CrossRef](#)]
51. OuYang, P.-Y.; Zhang, B.-Y.; Guo, J.-G.; Liu, J.-N.; Li, J.; Peng, Q.-H.; Yang, S.-S.; He, Y.; Liu, Z.-Q.; Zhao, Y.-N.; et al. Deep learning-based precise prediction and early detection of radiation-induced temporal lobe injury for nasopharyngeal carcinoma. *EClinicalMedicine* **2023**, *58*, 101930. [[CrossRef](#)]
52. OuYang, P.-Y.; He, Y.; Guo, J.-G.; Liu, J.-N.; Wang, Z.-L.; Li, A.; Li, J.; Yang, S.-S.; Zhang, X.; Fan, W.; et al. Artificial intelligence aided precise detection of local recurrence on MRI for nasopharyngeal carcinoma: A multicenter cohort study. *EClinicalMedicine* **2023**, *63*, 102202. [[CrossRef](#)] [[PubMed](#)]
53. Luo, X.; Liao, W.; He, Y.; Tang, F.; Wu, M.; Shen, Y.; Huang, H.; Song, T.; Li, K.; Zhang, S.; et al. Deep learning-based accurate delineation of primary gross tumor volume of nasopharyngeal carcinoma on heterogeneous magnetic resonance imaging: A large-scale and multi-center study. *Radiother. Oncol.* **2023**, *180*, 109480. [[CrossRef](#)] [[PubMed](#)]
54. Lu, S.; Xiao, X.; Yan, Z.; Cheng, T.; Tan, X.; Zhao, R.; Wu, H.; Shen, L.; Zhang, Z. Prognosis Forecast of Re-Irradiation for Recurrent Nasopharyngeal Carcinoma Based on Deep Learning Multi-Modal Information Fusion. *IEEE J. Biomed. Heal. Inform.* **2023**, *27*, 6088–6099. [[CrossRef](#)]
55. Liu, Y.; Sun, S.; Zhang, Y.; Huang, X.; Wang, K.; Qu, Y.; Chen, X.; Wu, R.; Zhang, J.; Luo, J.; et al. Predictive function of tumor burden-incorporated machine-learning algorithms for overall survival and their value in guiding management decisions in patients with locally advanced nasopharyngeal carcinoma. *J. Natl. Cancer Cent.* **2023**, *3*, 295–305. [[CrossRef](#)]
56. Liu, T.; Dong, D.; Zhao, X.; Ou, X.-M.; Yi, J.-L.; Guan, J.; Zhang, Y.; Xiao-Fei, L.; Xie, C.-M.; Luo, D.-H.; et al. Radiomic signatures reveal multiscale intratumor heterogeneity associated with tissue tolerance and survival in re-irradiated nasopharyngeal carcinoma: A multicenter study. *BMC Med.* **2023**, *21*, 464. [[CrossRef](#)] [[PubMed](#)]
57. Li, Y.; Weng, Y.; Huang, Z.; Pan, Y.; Cai, S.; Ding, Q.; Wu, Z.; Chen, X.; Lu, J.; Hu, D.; et al. Prognostic model on overall survival in elderly nasopharyngeal carcinoma patients: A recursive partitioning analysis identifying pre-treatment risk stratification. *Radiat. Oncol.* **2023**, *18*, 104. [[CrossRef](#)] [[PubMed](#)]

58. Li, S.; Zhang, W.; Liang, B.; Huang, W.; Luo, C.; Zhu, Y.; Kou, K.I.; Ruan, G.; Liu, L.; Zhang, G.; et al. A Rulefit-based prognostic analysis using structured MRI report to select potential beneficiaries from induction chemotherapy in advanced nasopharyngeal carcinoma: A dual-centre study. *Radiother. Oncol.* **2023**, *189*, 109943. [[CrossRef](#)]
59. Huang, Y.; Zhu, Y.; Yang, Q.; Luo, Y.; Zhang, P.; Yang, X.; Ren, J.; Ren, Y.; Lang, J.; Xu, G. Automatic tumor segmentation and metachronous single-organ metastasis prediction of nasopharyngeal carcinoma patients based on multi-sequence magnetic resonance imaging. *Front. Oncol.* **2023**, *13*, 953893. [[CrossRef](#)]
60. Huang, L.; Yang, Z.; Kang, M.; Ren, H.; Jiang, M.; Tang, C.; Hu, Y.; Shen, M.; Lin, H.; Long, L. Performance of Pretreatment MRI-Based Radiomics in Recombinant Human Endostatin Plus Concurrent Chemoradiotherapy Response Prediction in Nasopharyngeal Carcinoma: A Retrospective Study. *Technol. Cancer Res. Treat.* **2023**, *22*, 15330338231160619. [[CrossRef](#)]
61. Hua, H.-L.; Li, S.; Huang, H.; Zheng, Y.-F.; Li, F.; Li, S.-L.; Deng, Y.-Q.; Tao, Z.-Z. Deep learning for the prediction of residual tumor after radiotherapy and treatment decision-making in patients with nasopharyngeal carcinoma based on magnetic resonance imaging. *Quant. Imaging Med. Surg.* **2023**, *13*, 3569–3586. [[CrossRef](#)]
62. Hua, H.-L.; Deng, Y.-Q.; Li, S.; Li, S.-T.; Li, F.; Xiao, B.-K.; Huang, J.; Tao, Z.-Z. Deep Learning for Predicting Distant Metastasis in Patients with Nasopharyngeal Carcinoma Based on Pre-Radiotherapy Magnetic Resonance Imaging. *Comb. Chem. High Throughput Screen.* **2023**, *26*, 1351–1363. [[CrossRef](#)]
63. Guo, Y.; Dai, G.; Xiong, X.; Wang, X.; Chen, H.; Zhou, X.; Huang, W.; Chen, F. Intravoxel incoherent motion radiomics nomogram for predicting tumor treatment responses in nasopharyngeal carcinoma. *Transl. Oncol.* **2023**, *31*, 101648. [[CrossRef](#)]
64. Deng, Y.; Huang, Y.; Jing, B.; Wu, H.; Qiu, W.; Chen, H.; Li, B.; Guo, X.; Xie, C.; Sun, Y.; et al. Deep learning-based recurrence detector on magnetic resonance scans in nasopharyngeal carcinoma: A multicenter study. *Eur. J. Radiol.* **2023**, *168*, 111084. [[CrossRef](#)]
65. Zeng, F.; Lin, K.-R.; Jin, Y.-B.; Li, H.-J.; Quan, Q.; Su, J.-C.; Chen, K.; Zhang, J.; Han, C.; Zhang, G.-Y. MRI-based radiomics models can improve prognosis prediction for nasopharyngeal carcinoma with neoadjuvant chemotherapy. *Magn. Reson. Imaging* **2022**, *88*, 108–115. [[CrossRef](#)]
66. Yang, C.; Jiang, Z.; Cheng, T.; Zhou, R.; Wang, G.; Jing, D.; Bo, L.; Huang, P.; Wang, J.; Zhang, D.; et al. Radiomics for Predicting Response of Neoadjuvant Chemotherapy in Nasopharyngeal Carcinoma: A Systematic Review and Meta-Analysis. *Front. Oncol.* **2022**, *12*, 893103. [[CrossRef](#)] [[PubMed](#)]
67. Xie, F.; Zhao, Q.; Li, S.; Wu, S.; Li, J.; Li, H.; Chen, S.; Jiang, W.; Dong, A.; Wu, L.; et al. Establishment and validation of novel MRI radiomic feature-based prognostic models to predict progression-free survival in locally advanced rectal cancer. *Front. Oncol.* **2022**, *12*, 901287. [[CrossRef](#)] [[PubMed](#)]
68. Xi, Y.; Ge, X.; Ji, H.; Wang, L.; Duan, S.; Chen, H.; Wang, M.; Hu, H.; Jiang, F.; Ding, Z. Prediction of Response to Induction Chemotherapy Plus Concurrent Chemoradiotherapy for Nasopharyngeal Carcinoma Based on MRI Radiomics and Delta Radiomics: A Two-Center Retrospective Study. *Front. Oncol.* **2022**, *12*, 824509. [[CrossRef](#)] [[PubMed](#)]
69. Wang, Y.; Li, C.; Yin, G.; Wang, J.; Li, J.; Wang, P.; Bian, J. Extraction parameter optimized radiomics for neoadjuvant chemotherapy response prognosis in advanced nasopharyngeal carcinoma. *Clin. Transl. Radiat. Oncol.* **2021**, *33*, 37–44. [[CrossRef](#)]
70. Pei, W.; Wang, C.; Liao, H.; Chen, X.; Wei, Y.; Huang, X.; Liang, X.; Bao, H.; Su, D.; Jin, G. MRI-based random survival Forest model improves prediction of progression-free survival to induction chemotherapy plus concurrent Chemoradiotherapy in Locoregionally Advanced nasopharyngeal carcinoma. *BMC Cancer* **2022**, *22*, 739. [[CrossRef](#)]
71. Liu, L.; Pei, W.; Liao, H.; Wang, Q.; Gu, D.; Liu, L.; Su, D.; Jin, G. A Clinical-Radiomics Nomogram Based on Magnetic Resonance Imaging for Predicting Progression-Free Survival After Induction Chemotherapy in Nasopharyngeal Carcinoma. *Front. Oncol.* **2022**, *12*, 792535. [[CrossRef](#)]
72. Liao, H.; Chen, X.; Lu, S.; Jin, G.; Pei, W.; Li, Y.; Wei, Y.; Huang, X.; Wang, C.; Liang, X.; et al. MRI-Based Back Propagation Neural Network Model as a Powerful Tool for Predicting the Response to Induction Chemotherapy in Locoregionally Advanced Nasopharyngeal Carcinoma. *J. Magn. Reson. Imaging* **2022**, *56*, 547–559. [[CrossRef](#)]
73. Li, W.-Z.; Wu, G.; Li, T.-S.; Dai, G.-M.; Liao, Y.-T.; Yang, Q.-Y.; Chen, F.; Huang, W.-Y. Dynamic contrast-enhanced magnetic resonance imaging-based radiomics for the prediction of progression-free survival in advanced nasopharyngeal carcinoma. *Front. Oncol.* **2022**, *12*, 955866. [[CrossRef](#)]
74. Li, S.; Deng, Y.-Q.; Hua, H.-L.; Li, S.-L.; Chen, X.-X.; Xie, B.-J.; Zhu, Z.; Liu, R.; Huang, J.; Tao, Z.-Z. Deep learning for locally advanced nasopharyngeal carcinoma prognostication based on pre- and post-treatment MRI. *Comput. Methods Programs Biomed.* **2022**, *219*, 106785. [[CrossRef](#)] [[PubMed](#)]
75. Lam, S.-K.; Zhang, Y.; Zhang, J.; Li, B.; Sun, J.-C.; Liu, C.Y.-T.; Chou, P.-H.; Teng, X.; Ma, Z.-R.; Ni, R.-Y.; et al. Multi-Organ Omics-Based Prediction for Adaptive Radiation Therapy Eligibility in Nasopharyngeal Carcinoma Patients Undergoing Concurrent Chemoradiotherapy. *Front. Oncol.* **2022**, *11*, 792024. [[CrossRef](#)]
76. Jiang, T.; Tan, Y.; Nan, S.; Wang, F.; Chen, W.; Wei, Y.; Liu, T.; Qin, W.; Lu, F.; Jiang, F.; et al. Radiomics based on pretreatment MRI for predicting distant metastasis of nasopharyngeal carcinoma: A preliminary study. *Front. Oncol.* **2022**, *12*, 975881. [[CrossRef](#)]
77. Huang, Y.; Deng, Y.; Li, C.; Guo, X.; Lv, X. 662P Deep learning-enabled precise recurrence detection in nasopharyngeal carcinoma: A multicentre study. *Ann. Oncol.* **2022**, *33*, S845–S846. [[CrossRef](#)]
78. Hu, Q.; Wang, G.; Song, X.; Wan, J.; Li, M.; Zhang, F.; Chen, Q.; Cao, X.; Li, S.; Wang, Y. Machine Learning Based on MRI DWI Radiomics Features for Prognostic Prediction in Nasopharyngeal Carcinoma. *Cancers* **2022**, *14*, 3201. [[CrossRef](#)] [[PubMed](#)]

79. Hou, J.; Li, H.; Zeng, B.; Pang, P.; Ai, Z.; Li, F.; Lu, Q.; Yu, X. MRI-based radiomics nomogram for predicting temporal lobe injury after radiotherapy in nasopharyngeal carcinoma. *Eur. Radiol.* **2021**, *32*, 1106–1114. [[CrossRef](#)]
80. Feng, Q.; Liang, J.; Wang, L.; Ge, X.; Ding, Z.; Wu, H. A diagnosis model in nasopharyngeal carcinoma based on PET/MRI radiomics and semiquantitative parameters. *BMC Med. Imaging* **2022**, *22*, 150. [[CrossRef](#)]
81. Fang, Z.-Y.; Li, K.-Z.; Yang, M.; Che, Y.-R.; Luo, L.-P.; Wu, Z.-F.; Gao, M.-Q.; Wu, C.; Luo, C.; Lai, X.; et al. Integration of MRI-Based Radiomics Features, Clinicopathological Characteristics, and Blood Parameters: A Nomogram Model for Predicting Clinical Outcome in Nasopharyngeal Carcinoma. *Front. Oncol.* **2022**, *12*, 815952. [[CrossRef](#)]
82. Cao, X.; Chen, X.; Lin, Z.-C.; Liang, C.-X.; Huang, Y.-Y.; Cai, Z.-C.; Li, J.-P.; Gao, M.-Y.; Mai, H.-Q.; Li, C.-F.; et al. Add-on individualizing prediction of nasopharyngeal carcinoma using deep-learning based on MRI: A multicentre, validation study. *iScience* **2022**, *25*, 104841. [[CrossRef](#)]
83. Bao, D.; Zhao, Y.; Li, L.; Lin, M.; Zhu, Z.; Yuan, M.; Zhong, H.; Xu, H.; Zhao, X.; Luo, D. A MRI-based radiomics model predicting radiation-induced temporal lobe injury in nasopharyngeal carcinoma. *Eur. Radiol.* **2022**, *32*, 6910–6921. [[CrossRef](#)]
84. Bao, D.; Liu, Z.; Geng, Y.; Li, L.; Xu, H.; Zhang, Y.; Hu, L.; Zhao, X.; Zhao, Y.; Luo, D. Baseline MRI-based radiomics model assisted predicting disease progression in nasopharyngeal carcinoma patients with complete response after treatment. *Cancer Imaging* **2022**, *22*, 10. [[CrossRef](#)]
85. Zhong, L.; Dong, D.; Fang, X.; Zhang, F.; Zhang, N.; Zhang, L.; Fang, M.; Jiang, W.; Liang, S.; Li, C.; et al. A deep learning-based radiomic nomogram for prognosis and treatment decision in advanced nasopharyngeal carcinoma: A multicentre study. *EBioMedicine* **2021**, *70*, 103522. [[CrossRef](#)]
86. Zhang, L.; Wu, X.; Liu, J.; Zhang, B.; Mo, X.; Chen, Q.; Fang, J.; Wang, F.; Li, M.; Chen, Z.; et al. MRI-Based Deep-Learning Model for Distant Metastasis-Free Survival in Locoregionally Advanced Nasopharyngeal Carcinoma. *J. Magn. Reson. Imaging* **2020**, *53*, 167–178. [[CrossRef](#)] [[PubMed](#)]
87. Yongfeng, P.; Chuner, J.; Lei, W.; Fengqin, Y.; Zhimin, Y.; Zhenfu, F.; Haitao, J.; Yangming, J.; Fangzheng, W. The Usefulness of Pretreatment MR-Based Radiomics on Early Response of Neoadjuvant Chemotherapy in Patients With Locally Advanced Nasopharyngeal Carcinoma. *Oncol. Res.* **2020**, *28*, 605–613. [[CrossRef](#)]
88. Xu, H.; Liu, J.; Huang, Y.; Zhou, P.; Ren, J. MRI-based radiomics as response predictor to radiochemotherapy for metastatic cervical lymph node in nasopharyngeal carcinoma. *Br. J. Radiol.* **2021**, *94*, 20201212. [[CrossRef](#)]
89. Qiang, M.; Li, C.; Sun, Y.; Sun, Y.; Ke, L.; Xie, C.; Zhang, T.; Zou, Y.; Qiu, W.; Gao, M.; et al. A Prognostic Predictive System Based on Deep Learning for Locoregionally Advanced Nasopharyngeal Carcinoma. *JNCI J. Natl. Cancer Inst.* **2021**, *113*, 606–615. [[CrossRef](#)]
90. Mao, Y.; Wang, S.; Lydiatt, W.; Shah, J.P.; Colevas, A.D.; Lee, A.W.; O'Sullivan, B.; Guo, R.; Luo, W.; Chen, Y.; et al. Unambiguous advanced radiologic extranodal extension determined by MRI predicts worse outcomes in nasopharyngeal carcinoma: Potential improvement for future editions of N category systems. *Radiother. Oncol.* **2021**, *157*, 114–121. [[CrossRef](#)] [[PubMed](#)]
91. Li, Q.; Wang, T.; Huang, Y.; Li, Q.; Liu, P.; Grimm, R.; Fu, C.; Zhang, Y.; Gu, Y. Whole-Tumor Histogram and Texture Imaging Features on Magnetic Resonance Imaging Combined With Epstein-Barr Virus Status to Predict Disease Progression in Patients With Nasopharyngeal Carcinoma. *Front. Oncol.* **2021**, *11*, 610804. [[CrossRef](#)] [[PubMed](#)]
92. Lei, Y.; Li, Y.-Q.; Jiang, W.; Hong, X.-H.; Ge, W.-X.; Zhang, Y.; Hu, W.-H.; Wang, Y.-Q.; Liang, Y.-L.; Li, J.-Y.; et al. A Gene-Expression Predictor for Efficacy of Induction Chemotherapy in Locoregionally Advanced Nasopharyngeal Carcinoma. *JNCI J. Natl. Cancer Inst.* **2021**, *113*, 471–480. [[CrossRef](#)]
93. Kim, M.-J.; Choi, Y.; Sung, Y.E.; Lee, Y.S.; Kim, Y.-S.; Ahn, K.-J. Early risk-assessment of patients with nasopharyngeal carcinoma: The added prognostic value of MR-based radiomics. *Transl. Oncol.* **2021**, *14*, 101180. [[CrossRef](#)]
94. Kang, L.; Niu, Y.; Huang, R.; Lin, S.; Tang, Q.; Chen, A.; Fan, Y.; Lang, J.; Yin, G.; Zhang, P. Predictive Value of a Combined Model Based on Pre-Treatment and Mid-Treatment MRI-Radiomics for Disease Progression or Death in Locally Advanced Nasopharyngeal Carcinoma. *Front. Oncol.* **2021**, *11*, 774455. [[CrossRef](#)] [[PubMed](#)]
95. Hu, C.; Zheng, D.; Cao, X.; Pang, P.; Fang, Y.; Lu, T.; Chen, Y. Application Value of Magnetic Resonance Radiomics and Clinical Nomograms in Evaluating the Sensitivity of Neoadjuvant Chemotherapy for Nasopharyngeal Carcinoma. *Front. Oncol.* **2021**, *11*, 740776. [[CrossRef](#)] [[PubMed](#)]
96. Wu, S.; Li, H.; Dong, A.; Tian, L.; Ruan, G.; Liu, L.; Shao, Y. Differences in Radiomics Signatures Between Patients with Early and Advanced T-Stage Nasopharyngeal Carcinoma Facilitate Prognostication. *J. Magn. Reson. Imaging* **2021**, *54*, 854–865. [[CrossRef](#)] [[PubMed](#)]
97. Chen, X.; Li, Y.; Li, X.; Cao, X.; Xiang, Y.; Xia, W.; Li, J.; Gao, M.; Sun, Y.; Liu, K.; et al. An interpretable machine learning prognostic system for locoregionally advanced nasopharyngeal carcinoma based on tumor burden features. *Oral Oncol.* **2021**, *118*, 105335. [[CrossRef](#)] [[PubMed](#)]
98. Bao, D.; Zhao, Y.; Liu, Z.; Zhong, H.; Geng, Y.; Lin, M.; Li, L.; Zhao, X.; Luo, D. Prognostic and predictive value of radiomics features at MRI in nasopharyngeal carcinoma. *Discov. Oncol.* **2021**, *12*, 63. [[CrossRef](#)] [[PubMed](#)]
99. Zhong, L.-Z.; Fang, X.-L.; Dong, D.; Peng, H.; Fang, M.-J.; Huang, C.-L.; He, B.-X.; Lin, L.; Ma, J.; Tang, L.-L.; et al. A deep learning MR-based radiomic nomogram may predict survival for nasopharyngeal carcinoma patients with stage T3N1M0. *Radiother. Oncol.* **2020**, *151*, 1–9. [[CrossRef](#)] [[PubMed](#)]

100. Zhong, L.; Dong, D.; Tang, L.; Han, S.; Tian, J. Abstract 5430: Deep learning-based prognosis prediction in T3N1 nasopharyngeal carcinoma patients treated with induction chemotherapy followed by concurrent chemoradiotherapy. *Cancer Res* **2020**, *80* (Suppl. S16), 5430. [[CrossRef](#)]
101. Zhao, L.; Gong, J.; Xi, Y.; Xu, M.; Li, C.; Kang, X.; Yin, Y.; Qin, W.; Yin, H.; Shi, M. MRI-based radiomics nomogram may predict the response to induction chemotherapy and survival in locally advanced nasopharyngeal carcinoma. *Eur. Radiol.* **2019**, *30*, 537–546. [[CrossRef](#)]
102. Zhang, L.; Ye, Z.; Ruan, L.; Jiang, M. Pretreatment MRI-Derived Radiomics May Evaluate the Response of Different Induction Chemotherapy Regimens in Locally advanced Nasopharyngeal Carcinoma. *Acad. Radiol.* **2020**, *27*, 1655–1664. [[CrossRef](#)] [[PubMed](#)]
103. Wang, Y.; Yin, G.; Wang, J.; Lang, J.; Li, C. Multi-sequence MRI based Radiomics Model in Predicting Efficacy of Neoadjuvant Chemotherapy for Nasopharyngeal Carcinoma. *Endocrine* **2020**, *108*, S32–S33. [[CrossRef](#)]
104. Wang, J.; Liu, R.; Zhao, Y.; Nantavithya, C.; Elhalawani, H.; Zhu, H.; Mohamed, A.S.R.; Fuller, C.D.; Kannarunimit, D.; Yang, P.; et al. A predictive model of radiation-related fibrosis based on the radiomic features of magnetic resonance imaging and computed tomography. *Transl. Cancer Res.* **2020**, *9*, 4726–4738. [[CrossRef](#)] [[PubMed](#)]
105. Shen, H.; Wang, Y.; Liu, D.; Lv, R.; Huang, Y.; Peng, C.; Jiang, S.; Wang, Y.; He, Y.; Lan, X.; et al. Predicting Progression-Free Survival Using MRI-Based Radiomics for Patients With Nonmetastatic Nasopharyngeal Carcinoma. *Front. Oncol.* **2020**, *10*, 618. [[CrossRef](#)] [[PubMed](#)]
106. Jing, B.; Deng, Y.; Zhang, T.; Hou, D.; Li, B.; Qiang, M.; Liu, K.; Ke, L.; Li, T.; Sun, Y.; et al. Deep learning for risk prediction in patients with nasopharyngeal carcinoma using multi-parametric MRIs. *Comput. Methods Programs Biomed.* **2020**, *197*, 105684. [[CrossRef](#)] [[PubMed](#)]
107. Feng, Q.; Liang, J.; Wang, L.; Niu, J.; Ge, X.; Pang, P.; Ding, Z. Radiomics Analysis and Correlation With Metabolic Parameters in Nasopharyngeal Carcinoma Based on PET/MR Imaging. *Front. Oncol.* **2020**, *10*, 01619. [[CrossRef](#)] [[PubMed](#)]
108. Cui, C.; Wang, S.; Zhou, J.; Dong, A.; Xie, F.; Li, H.; Liu, L. Machine Learning Analysis of Image Data Based on Detailed MR Image Reports for Nasopharyngeal Carcinoma Prognosis. *BioMed Res. Int.* **2020**, *2020*, 8068913. [[CrossRef](#)] [[PubMed](#)]
109. Akram, F.; Koh, P.E.; Wang, F.; Zhou, S.; Tan, S.H.; Paknezhad, M.; Park, S.; Henedige, T.; Thng, C.H.; Lee, H.K.; et al. Exploring MRI based radiomics analysis of intratumoral spatial heterogeneity in locally advanced nasopharyngeal carcinoma treated with intensity modulated radiotherapy. *PLoS ONE* **2020**, *15*, e0240043. [[CrossRef](#)]
110. Zhuo, E.H.; Zhang, W.J.; Li, H.J.; Zhang, G.Y.; Jing, B.Z.; Zhou, J.; Cui, C.Y.; Chen, M.Y.; Sun, Y.; Liu, L.Z.; et al. Radiomics on multi-modalities MR sequences can subtype patients with non-metastatic nasopharyngeal carcinoma (NPC) into distinct survival subgroups. *Eur. Radiol.* **2019**, *29*, 5590–5599. [[CrossRef](#)]
111. Zhang, L.; Zhou, H.; Gu, D.; Tian, J.; Zhang, B.; Dong, D.; Mo, X.; Liu, J.; Luo, X.; Pei, S.; et al. Radiomic Nomogram: Pretreatment Evaluation of Local Recurrence in Nasopharyngeal Carcinoma based on MR Imaging. *J. Cancer* **2019**, *10*, 4217–4225. [[CrossRef](#)]
112. Zhang, L.; Dong, D.; Li, H.; Tian, J.; Ouyang, F.; Mo, X.; Zhang, B.; Luo, X.; Lian, Z.; Pei, S.; et al. Development and validation of a magnetic resonance imaging-based model for the prediction of distant metastasis before initial treatment of nasopharyngeal carcinoma: A retrospective cohort study. *EBioMedicine* **2019**, *40*, 327–335. [[CrossRef](#)]
113. Yu, T.-T.; Lam, S.-K.; To, L.-H.; Tse, K.-Y.; Cheng, N.-Y.; Fan, Y.-N.; Lo, C.-L.; Or, K.-W.; Chan, M.-L.; Hui, K.-C.; et al. Pretreatment Prediction of Adaptive Radiation Therapy Eligibility Using MRI-Based Radiomics for Advanced Nasopharyngeal Carcinoma Patients. *Front. Oncol.* **2019**, *9*, 1050. [[CrossRef](#)]
114. Yang, K.; Tian, J.; Zhang, B.; Li, M.; Xie, W.; Zou, Y.; Tan, Q.; Liu, L.; Zhu, J.; Shou, A.; et al. A multidimensional nomogram combining overall stage, dose volume histogram parameters and radiomics to predict progression-free survival in patients with locoregionally advanced nasopharyngeal carcinoma. *Oral Oncol.* **2019**, *98*, 85–91. [[CrossRef](#)] [[PubMed](#)]
115. Nair, J.K.R.; Vallières, M.; Mascarella, M.A.; El Sabbagh, N.; Duchatellier, C.F.; Zeitouni, A.; Shenouda, G.; Chankowsky, J. Magnetic Resonance Imaging Texture Analysis Predicts Recurrence in Patients with Nasopharyngeal Carcinoma. *Can. Assoc. Radiol. J.* **2019**, *70*, 394–402. [[CrossRef](#)]
116. Qiang, M.; Lv, X.; Li, C.; Liu, K.; Chen, X.; Guo, X. Deep learning in nasopharyngeal carcinoma: A retrospective cohort study of 3D convolutional neural networks on magnetic resonance imaging. *Ann. Oncol.* **2019**, *30*, v471. [[CrossRef](#)]
117. Mao, J.; Fang, J.; Duan, X.; Yang, Z.; Cao, M.; Zhang, F.; Lu, L.; Zhang, X.; Wu, X.; Ding, Y.; et al. Predictive value of pretreatment MRI texture analysis in patients with primary nasopharyngeal carcinoma. *Eur. Radiol.* **2019**, *29*, 4105–4113. [[CrossRef](#)] [[PubMed](#)]
118. Liang, Z.; Zhang, F.; Tan, L.; Lin, L.; Lenkiewicz, J.; Wang, H.; Ong, E.; Kusumawidjaja, G.; Phua, J.; Tan, T.; et al. Radio-Transcriptomic phenotypes predict radioresistance in nasopharyngeal carcinoma. *Endocrine* **2019**, *105*, E388–E389. [[CrossRef](#)]
119. Liang, Z.-G.; Tan, H.Q.; Zhang, F.; Tan, L.K.R.; Lin, L.; Lenkiewicz, J.; Wang, H.; Ong, E.H.W.; Kusumawidjaja, G.; Phua, J.H.; et al. Comparison of radiomics tools for image analyses and clinical prediction in nasopharyngeal carcinoma. *Br. J. Radiol.* **2019**, *92*, 20190271. [[CrossRef](#)]
120. Li, S.; Wang, K.; Hou, Z.; Yang, J.; Ren, W.; Gao, S.; Meng, F.; Wu, P.; Liu, B.; Liu, J.; et al. Use of Radiomics Combined With Machine Learning Method in the Recurrence Patterns After Intensity-Modulated Radiotherapy for Nasopharyngeal Carcinoma: A Preliminary Study. *Front. Oncol.* **2018**, *8*, 648. [[CrossRef](#)] [[PubMed](#)]
121. Du, R.; Lee, V.H.; Yuan, H.; Lam, K.-O.; Pang, H.H.; Chen, Y.; Lam, E.Y.; Khong, P.-L.; Lee, A.W.; Kwong, D.L.; et al. Radiomics Model to Predict Early Progression of Nonmetastatic Nasopharyngeal Carcinoma after Intensity Modulation Radiation Therapy: A Multicenter Study. *Radiol. Artif. Intell.* **2019**, *1*, e180075. [[CrossRef](#)]

122. Dong, D.; Zhang, F.; Zhong, L.-Z.; Fang, M.-J.; Huang, C.-L.; Yao, J.-J.; Sun, Y.; Tian, J.; Ma, J.; Tang, L.-L. Development and validation of a novel MR imaging predictor of response to induction chemotherapy in locoregionally advanced nasopharyngeal cancer: A randomized controlled trial substudy (NCT01245959). *BMC Med.* **2019**, *17*, 190. [[CrossRef](#)] [[PubMed](#)]
123. Choi, C.; Chau, T.; Chau, S.; Lam, K.; Chan, S.; Tong, C.; Chan, W.; Kwong, D.; Leung, T.; Luk, M.; et al. Development and validation of M1 substages for previously untreated metastatic nasopharyngeal carcinoma. *Ann. Oncol.* **2019**, *30*, ix100. [[CrossRef](#)]
124. Zhao, L.; Gong, J.; Yin, H.; Qin, W.; Shi, M. Multiparametric MRI based radiomics for the prediction of induction chemotherapy response and survival in locally advanced nasopharyngeal carcinoma. *Endocrine* **2018**, *102*, S127. [[CrossRef](#)]
125. Wang, G.; He, L.; Yuan, C.; Huang, Y.; Liu, Z.; Liang, C. Pretreatment MR imaging radiomics signatures for response prediction to induction chemotherapy in patients with nasopharyngeal carcinoma. *Eur. J. Radiol.* **2018**, *98*, 100–106. [[CrossRef](#)] [[PubMed](#)]
126. Qin, Y.; Yu, X.; Hou, J.; Hu, Y.; Li, F.; Wen, L.; Lu, Q.; Fu, Y.; Liu, S. Predicting chemoradiotherapy response of nasopharyngeal carcinoma using texture features based on intravoxel incoherent motion diffusion-weighted imaging. *Medicine* **2018**, *97*, e11676. [[CrossRef](#)] [[PubMed](#)]
127. Zhang, B.; Ouyang, F.; Gu, D.; Dong, Y.; Zhang, L.; Mo, X.; Huang, W.; Zhang, S. Advanced nasopharyngeal carcinoma: Pre-treatment prediction of progression based on multi-parametric MRI radiomics. *Oncotarget* **2017**, *8*, 72457–72465. [[CrossRef](#)] [[PubMed](#)]
128. Smekens, F.; Chautard, E.; Debiton, E.; Dedieu, V.; Degoul, F.; Hérault, J.; Montarou, G.; Vert, P.-E.; Maigne, L. Scientific Abstracts and Sessions. *Med. Phys.* **2017**, *44*, 2721–3318. [[CrossRef](#)]
129. Liu, J.; Mao, Y.; Li, Z.; Zhang, D.; Zhang, Z.; Hao, S.; Li, B. Use of texture analysis based on contrast-enhanced MRI to predict treatment response to chemoradiotherapy in nasopharyngeal carcinoma. *J. Magn. Reson. Imaging* **2016**, *44*, 445–455. [[CrossRef](#)] [[PubMed](#)]
130. Farhidzadeh, H.; Kim, J.Y.; Scott, J.G.; Goldgof, D.B.; Hall, L.O.; Harrison, L.B. Classification of progression free survival with nasopharyngeal carcinoma tumors. In *Medical Imaging 2016: Computer-Aided Diagnosis*; SPIE: Bellingham, WA, USA, 2016.
131. von Hippel, P.T. The heterogeneity statistic I2 can be biased in small meta-analyses. *BMC Med. Res. Methodol.* **2015**, *15*, 35. [[CrossRef](#)]
132. Khanfari, H.; Mehranfar, S.; Cheki, M.; Sadr, M.M.; Moniri, S.; Heydarheydari, S.; Rezaeijo, S.M. Exploring the efficacy of multi-flavored feature extraction with radiomics and deep features for prostate cancer grading on mpMRI. *BMC Med. Imaging* **2023**, *23*, 195. [[CrossRef](#)]
133. Reginelli, A.; Nardone, V.; Giacobbe, G.; Belfiore, M.P.; Grassi, R.; Schettino, F.; Del Canto, M.; Grassi, R.; Cappabianca, S. Radiomics as a New Frontier of Imaging for Cancer Prognosis: A Narrative Review. *Diagnostics* **2021**, *11*, 1796. [[CrossRef](#)] [[PubMed](#)]

Disclaimer/Publisher’s Note: The statements, opinions and data contained in all publications are solely those of the individual author(s) and contributor(s) and not of MDPI and/or the editor(s). MDPI and/or the editor(s) disclaim responsibility for any injury to people or property resulting from any ideas, methods, instructions or products referred to in the content.